



NAVAL POSTGRADUATE SCHOOL

MONTEREY, CALIFORNIA

THESIS

**ASSESSING THE PERFORMANCE OF OMNI-
DIRECTIONAL RECEIVERS FOR PASSIVE ACOUSTIC
DETECTION OF VOCALIZING ODONTOCETES**

by

John M. Daziens

June 2004

Thesis Advisor:

Ching-Sang Chiu

Co-Advisor:

Curtis A. Collins

:

Approved for public release, distribution unlimited

THIS PAGE INTENTIONALLY LEFT BLANK

REPORT DOCUMENTATION PAGE			Form Approved OMB No. 0704-0188	
Public reporting burden for this collection of information is estimated to average 1 hour per response, including the time for reviewing instruction, searching existing data sources, gathering and maintaining the data needed, and completing and reviewing the collection of information. Send comments regarding this burden estimate or any other aspect of this collection of information, including suggestions for reducing this burden, to Washington headquarters Services, Directorate for Information Operations and Reports, 1215 Jefferson Davis Highway, Suite 1204, Arlington, VA 22202-4302, and to the Office of Management and Budget, Paperwork Reduction Project (0704-0188) Washington DC 20503.				
1. AGENCY USE ONLY (Leave blank)	2. REPORT DATE June 2004	3. REPORT TYPE AND DATES COVERED Master's Thesis		
4. TITLE AND SUBTITLE: Assessing the Performance of Omni-Directional Receivers for Passive Acoustic Detection of Vocalizing Odontocetes			5. FUNDING NUMBERS	
6. AUTHOR(S) John M. Daziens				
7. PERFORMING ORGANIZATION NAME(S) AND ADDRESS(ES) Naval Postgraduate School Monterey, CA 93943-5000			8. PERFORMING ORGANIZATION REPORT NUMBER	
9. SPONSORING /MONITORING AGENCY NAME(S) AND ADDRESS(ES) Chief of Naval Operations, Environmental Readiness Division (N45) Crystal Plaza 5 Arlington, VA			10. SPONSORING/MONITORING AGENCY REPORT NUMBER	
11. SUPPLEMENTARY NOTES The views expressed in this thesis are those of the author and do not reflect the official policy or position of the Department of Defense or the U.S. Government.				
12a. DISTRIBUTION / AVAILABILITY STATEMENT Approved for public release, distribution unlimited			12b. DISTRIBUTION CODE	
13. ABSTRACT (maximum 200 words) This study sought to experimentally quantify the sonar performance of omni-directional receivers as a means to passively detect vocalizing Odontocetes. To accomplish this objective, controlled experiments using a calibrated mid-frequency sound source were conducted on the San Clemente Island Underwater Range (SCIUR) in July 2002. Six Odontocete signals were selected for transmission: 2 orca and 2 pilot whale whistles, and sperm whale and Risso's dolphin clicks. Several hundred iterations of each signal were broadcast at stations 300 m to 12,000 m from the range's moored, three-element array. Statistical analyses were performed on the output of an energy and matched filter detector to quantify detection probability (P(D)) and range limits as a function of false alarm rate (P(FA)), signal type, and signal to noise ratio (SNR). The matched filter was generally the superior performer, detecting the orca2 and pilot1 whistles beyond 5000 m with a 90% P(D), 1% P(FA), and source level (SL) of 140 dB re 1 μ Pa. For the same conditions, the orca1 and sperm whale calls were detected at 1500 m, but the pilot2 and Risso's dolphin signals were not detected at the peak realized SNR of (-2) dB. The energy detector had no detections with a 90% P(D) and 1% P(FA) at this (-2) dB SNR, but all signals except one orca whistle were detectable beyond 1000 m with a 50% P(D) and 1% P(FA). The sperm whale was the exceptional energy detector performer, with detection ranges exceeding 7 km (140 dB re 1 μ Pa SL) at the 50% P(D) and 1% P(FA).				
14. SUBJECT TERMS Oceanography, Acoustics, Marine Mammals, Odontocetes, Whales			15. NUMBER OF PAGES 57	
			16. PRICE CODE	
17. SECURITY CLASSIFICATION OF REPORT Unclassified	18. SECURITY CLASSIFICATION OF THIS PAGE Unclassified	19. SECURITY CLASSIFICATION OF ABSTRACT Unclassified	20. LIMITATION OF ABSTRACT UL	

THIS PAGE INTENTIONALLY LEFT BLANK

Approved for public release, distribution unlimited

**ASSESSING THE PERFORMANCE OF OMNI-DIRECTIONAL RECEIVERS
FOR PASSIVE ACOUSTIC DETECTION OF VOCALIZING ODONTOCETES**

John M. Daziens
Lieutenant Commander, United States Navy
B.S. Ocean Engineering, United States Naval Academy, 1990
M.S. Environmental Science, Johns Hopkins University, 1999

Submitted in partial fulfillment of the
requirements for the degree of

**MASTER OF SCIENCE IN METEOROLOGY AND PHYSICAL
OCEANOGRAPHY**

from the

**NAVAL POSTGRADUATE SCHOOL
June 2004**

Author: John M. Daziens

Approved by: Ching-Sang Chiu
Thesis Advisor

Curtis A. Collins
Co-Advisor

Mary L. Batteen
Chairperson, Department of Oceanography

THIS PAGE INTENTIONALLY LEFT BLANK

ABSTRACT

Acoustic detection and localization of marine mammals will assist mitigation efforts for various Naval and scientific missions that may impact protected species. This study sought to experimentally quantify the sonar performance of omni-directional receivers as a means to passively detect vocalizing Odontocetes in coastal waters. To accomplish this objective, controlled experiments using a calibrated mid-frequency sound source were conducted on the San Clemente Island Underwater Range (SCIUR) in July 2002. Six Odontocete signals were selected for transmission based upon availability and quality of archived recordings: 2 orca and 2 pilot whale whistles, and sperm whale and Risso's dolphin clicks. Several hundred iterations of each signal were broadcast from *R/V Point Sur* at stations 300 m to 12,000 m from the range's moored, three-element array. Statistical analyses were performed on the output of an energy and matched filter detector to quantify detection probability and range limits as a function of false alarm rate, signal type, and signal to noise ratio. The matched filter generally outperformed the energy detector with respect to the required signal to noise ratios and maximum detection range for given probabilities of detection $P(D)$ and false alarm rate $P(FA)$. The matched filter detected the orca2 and pilot1 whistles beyond 5000 m with a 90% $P(D)$, 1% $P(FA)$, and source level (SL) of 140 dB re 1 μ Pa. For the same conditions, the orca1 and sperm whale calls were detected at 1500 m, but the pilot2 and Risso's dolphin signals were not detected at the peak realized SNR of -2 dB. The energy detector had no detections with a 90% $P(D)$ and 1% $P(FA)$ at this -2 dB SNR, but all signals except one orca whistle were detectable beyond 1000 m with a 50% $P(D)$ and 1% $P(FA)$. The sperm whale was the exceptional energy detector performer, with detection ranges exceeding 7 km (140 dB re 1 μ Pa SL) at the 50% $P(D)$ and 1% $P(FA)$.

THIS PAGE INTENTIONALLY LEFT BLANK

TABLE OF CONTENTS

I.	BACKGROUND AND INTRODUCTION.....	1
A.	INTRODUCTION.....	1
B.	ASSUMPTIONS.....	3
II.	METHODS.....	5
A.	DATA COLLECTION.....	5
B.	SIGNAL SELECTION.....	6
C.	ENVIRONMENTAL CONDITIONS AND BACKGROUND NOISE.....	8
D.	DATA ANALYSIS.....	10
1.	Matched Filter Detector.....	10
2.	Energy Detector.....	13
3.	Ambient Noise Analysis.....	14
4.	Source Level Calculations.....	19
III.	RESULTS AND ANALYSIS.....	23
A.	SOURCE LEVELS.....	23
B.	CURVE FITTING.....	24
C.	DETECTOR PERFORMANCE CURVES.....	28
1.	Matched Filter and Energy Detector Performance.....	29
a.	<i>Orca1 Whistle</i>	30
b.	<i>Orca2 Whistle</i>	31
c.	<i>Pilot1 Whistle</i>	32
d.	<i>Pilot2 Whistle</i>	33
e.	<i>Risso's Dolphin Click</i>	34
f.	<i>Sperm Whale Click</i>	35
2.	Comparison of Detector Performance.....	36
D.	SIGNAL CLASSIFICATION.....	37
IV.	CONCLUSIONS.....	41
	LIST OF REFERENCES.....	43
	INITIAL DISTRIBUTION LIST.....	45

THIS PAGE INTENTIONALLY LEFT BLANK

ACKNOWLEDGMENTS

This work could not have been possible without the guidance, assistance, and motivation of several dedicated individuals. Professors Collins, Batteen, and C-S Chiu were instrumental in the revision, editing, and massaging of the final version. Tarry Rago, Bob Creasey, and Dick Lind gathered and processed the environmental data for the three days of at sea experiments. Anurag Kumar and Chris Miller were ever present as sounding boards and mentors while weaving through the data analysis, as well as providing the technical expertise for computer programming and MATLAB manipulations. Lieutenant Commander Dave Brown of the NPS Meteorology Department was a key ally, keeping the author abreast of the many mitigation issues pertaining to this research. And finally my warmest regards and thanks to my family, friends, and loving wife Leah who were always supportive and full of good spirits during this project.

THIS PAGE INTENTIONALLY LEFT BLANK

I. BACKGROUND AND INTRODUCTION

A. INTRODUCTION

In July 2002, a three-day playback experiment was conducted off the California coast to quantify the detection and classification capabilities and range limits of omni-directional hydrophones and processing techniques in the detection of Odontocete vocalizations.

Traditionally the localization and tracking of Cetaceans has been done through visual survey methods. The feasibility of detecting, localizing, and tracking Odontocetes with hydrophones and passive arrays to augment visual whale sightings at short distances has been demonstrated by Borsani, et al. (2003). Monitoring of baleen whales using low-frequency sounds has been proven effective at long ranges by Chiu and Miller (1992) and Hager (1997), among others. Acoustic detection and localization of marine mammals will assist mitigation efforts for various naval and scientific missions that may impact protected species. Anthropogenic noises previously have been proven to affect various marine mammals. Shipping traffic, active sonar, underwater detonations, and air guns are among the noise sources of concern for marine mammal mitigation (Richardson, et al., 1995). Standoff distances are a common proviso to mitigate environmental impacts to marine mammals. Acoustic methods may be a legitimate form of mitigation to augment visual search procedures, especially during periods of low or restricted visibility.

In order to apply acoustic detection methods for reliable mitigation or marine mammal detection purposes, the receiver operating characteristic (ROC) curves must be established. The ROC curves provide the signal detection probabilities as functions of the received signal to noise ratio (SNR) and false alarm rates for a detector. Given a known source level (SL) and measured environmental noise condition, the SNR can be correlated to the source-to-receiver distance for measuring the standoff range. In light of this, there is a

need to establish quantitative predictions of which Odontocete signals are detectable, the detection reliability, and achievable detection distances.

Odontocetes are the suborder of toothed whales within the order Cetacea (Orr, 1972). Mid-frequency signals (1-8 kHz) were used in this trial due to hardware constraints. Most Odontoceti whales vocalize above 1.5 kHz. The propagation of these signals depends strongly upon frequency, with the noise levels decreasing at higher frequencies while the attenuation and scattering losses increase. Chemical relaxation, seawater absorption, volume scattering, and boundary roughness effects exponentially increase to impede propagation of frequencies greater than 10 kHz. Boric acid relaxation affects frequencies around 1 kHz, while magnesium sulfate ($MgSO_4$) ionic relaxation is the dominant absorption factor between 10-200 kHz. The attenuation coefficient is the sum of these relaxation terms and the viscosity effects (Medwin and Clay, 1998):

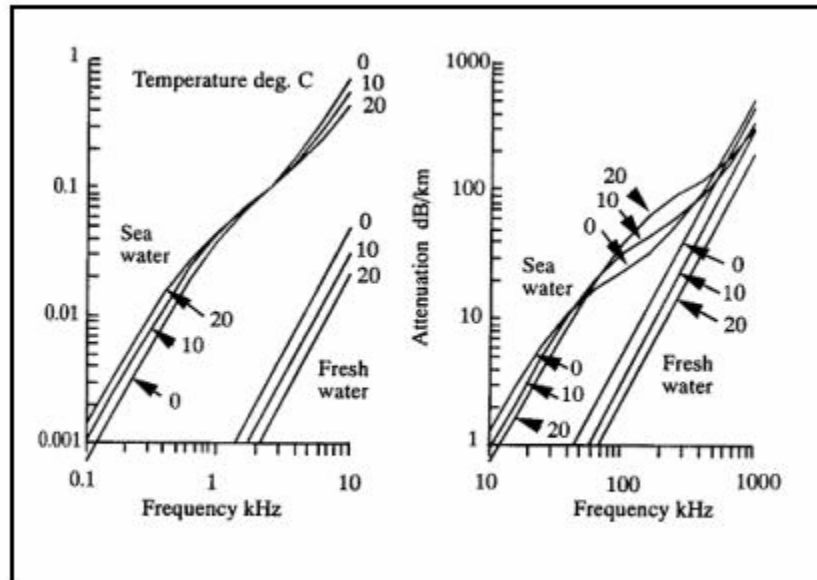


Figure 1: Sound pressure attenuation rate in dB/km at temperatures 0°, 10°, and 20° C for fresh and sea water (depth $z = 0$ m; sea water pH=8 and S=35 ppt) (Medwin and Clay, 1998).

Simulated Odontocete transmissions were broadcast at controlled distances and recorded by a moored, vertical line array on the San Clemente

Underwater Instrument Range (SCIUR). Accumulated time series of this data were then analyzed using energy and matched filter (correlation) detectors. Statistical analysis of the detector outputs quantified detection probability and range limits at the selected source level, as a function of false alarm rate, signal type, and signal to noise ratio. The techniques and results produced by this experiment were intended to be generic, and are easily applicable to sonobuoys or fixed hydrophones.

B. ASSUMPTIONS

Several assumptions were required based upon hardware constraints and existing gaps in currently published scientific research. Detection of vocalizing Odontocetes is the primary constraint upon this experiment; detection of non-singing marine mammals is beyond the scope of this project. Hardware constraints limited the intensity and frequency ranges of the replicated source signals. Source levels were voltage limited to approximately 140 dB re: 1 μ Pa, below the peak-to-peak source levels of many Odontocetes cited in current literature. Despite this limitation, generation of detection probabilities at varying false alarm rates using a signal-to-noise ratio (SNR) approach enables the end user to apply desired source levels to determine detection ranges. Due to the attenuation and scattering limits upon higher frequency propagations, the 1-8 kHz bandwidth analyzed was assumed to adequately represent the primary features and characteristics of the selected Odontocete signals. Omni-directional signals were broadcast and analyzed, and no attempt was made to simulate the beamforming characteristics attributed to echolating species (Purvis and Pilleri, 1983). Also, this research does not address bioacoustic variations of the discrete whale signals, and no variation of signal source levels or of the chosen whistle and click wave patterns was performed. Variations in call rates or patterns due to marine mammal behavioral patterns during transits, feeding, or diurnal or seasonal cycles are beyond the scope of this project.

THIS PAGE INTENTIONALLY LEFT BLANK

II. METHODS

A. DATA COLLECTION

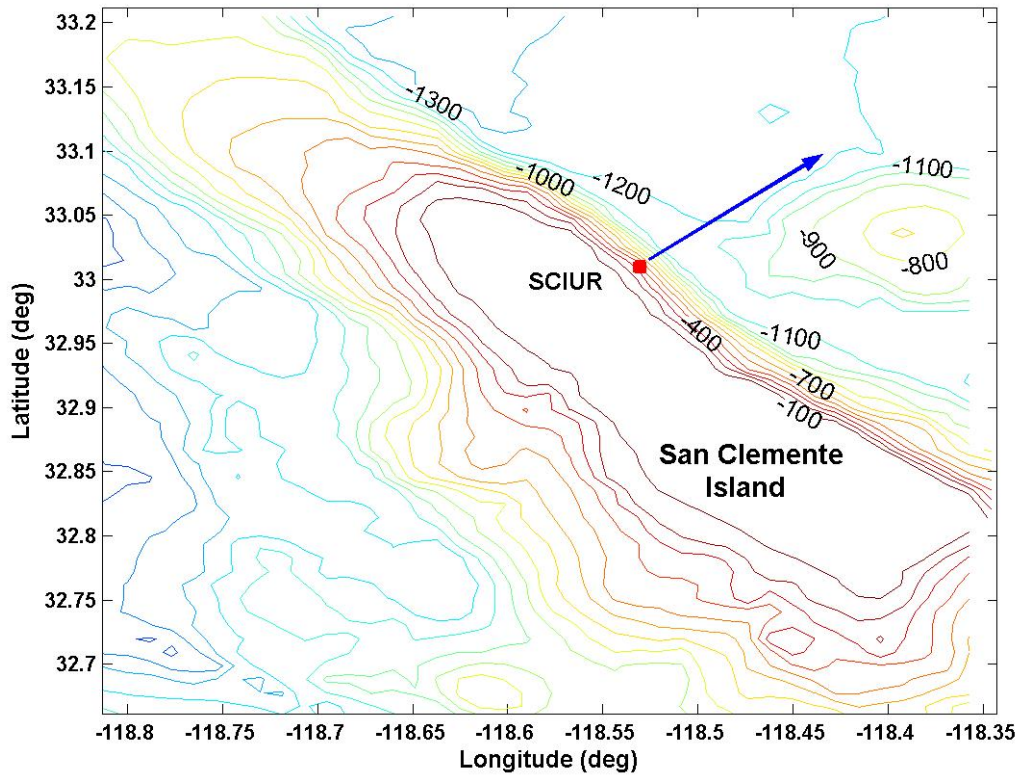


Figure 2: San Clemente Island Underwater Range (SCIUR) off southern California. Ship track (blue line) is indicated relative to the receiver array (red box). Depth contours are plotted in 100 meter increments (Miller and Kumar, 2003).

A playback experiment was conducted in July 2002 at the U.S. Navy's San Clemente Island Underwater Range (SCIUR) to quantify the passive acoustic detection performance of omni-directional receivers against vocalizing Odontocetes. The primary receivers analyzed during this project were the three elements of the SCIUR moored vertical line array, comprised of ITC-6050C hydrophones with bandwidths of 20 Hz to 75 kHz and sensitivities of -161 dB re $1\text{V}/\mu\text{Pa}$. The elements were situated at depths of 75.3, 136.6, and 165.8 m,

hereafter designated “channel 1,” “channel 2,” and “channel 3” respectively. Acoustic data from these hydrophones was recorded throughout the three-day project, and stored in one minute data acquisition files using a sampling rate of 33 kHz (Miller and Kumar, 2003).

AN/SSQ-57B sonobuoys were deployed along the broadcast path with GPS receivers fixing their position. Analysis of the recorded sonobuoy data is beyond the scope of this paper, although the same techniques are applicable to that dataset.

Over the course of three days on the range, five runs were conducted. Within these runs, six selected signals were broadcast in sets of fifty transmissions each at pre-set stations varying in distances from one to twelve kilometers. A one second pause was placed between individual transmissions, and a three second pause with a 3 kHz tone between sets of whale calls. GPS tracking was used to fix the transmissions, generated by a type G34 transducer built by the Naval Undersea Warfare Center’s Underwater Sound Reference Division. Though rated to only 5 kHz, testing of the G34 revealed a smooth and gradual response curve through the 8 kHz peak frequency utilized in this experiment. The maximum observed G34 broadband source levels were approximately 140 dB re 1 μ Pa due to system setup voltage limitations. Primary transmission depth was 30 m. A calibrated High Tech HTI-96-MIN hydrophone with a frequency range of 0 to 30 kHz and sensitivity of -164.8 db Volts/ μ Pa was tethered astern the *R/V Point Sur* to measure the source signal transmissions (Miller and Kumar, 2003).

B. SIGNAL SELECTION

A variety of signals – different species and an assortment of “whistles” and “clicks” – was desired to represent the marine mammals within the suborder Odontocete. “Whistles” are sets of narrowband, near tonal sounds predominately used as “signature calls,” identifying individual whales within the groups and possibly serving as communication tools. Acoustic energy for these

calls is generally focused below 20 kHz, and may exhibit trilled, ascending or descending frequency waveforms. Pulsed sounds such as grunts, cries, and barks are termed “clicks.” These are commonly produced by sperm and killer whales, and have been attributed to pod and caller identification. Sperm whale clicks range from <100 Hz to 30 kHz, with most of the energy centered within the 2-4 kHz bandwidth, and are repeated up to 90 times per second. Ultra high frequency echolocation clicks are also common to Odontocetes, but were beyond the scope of this analysis (Richardson, et al., 1995).

To best meet the primary objective of determining detection probabilities at given false alarm rates, a large sample size of signal and noise realizations was desired. A limit of six signals was set as a compromise between the whale call variability and a maximized data sample size to meet the constraints of the experiment’s limited ship time. Availability of adequate signals limited the whale call selection process, as recorded samples devoid of noise were required to provide clear playback sources for the statistical analysis. Waveform complexity was also a decision factor, whereby the major characteristics of the signal had to lie within the 1-8 kHz bandwidth targeted for analysis.

Four whistles and two clicks were chosen: two orca whistles, two pilot whale whistles, and the Risso’s dolphin and sperm whale clicks. These whale calls represent the larger Odontocetes, and all are native to the northern pacific waters. The spectrograms for these signals are shown in Figure 3.

Each recorded whale signal was filtered using a 4th order Butterworth filter with a passband between 1-8 kHz, and peak-peak normalized to 0.99 amplitude to prevent clipping of the waveform during transmission by a 1.0 Volt amplifier. For purposes of this experiment, an **ensemble** or **signal train** will describe a set of fifty contiguous calls, and a **broadcast** will encompass the complete collection of the six ensembles at a given station (Garcia, 2002).

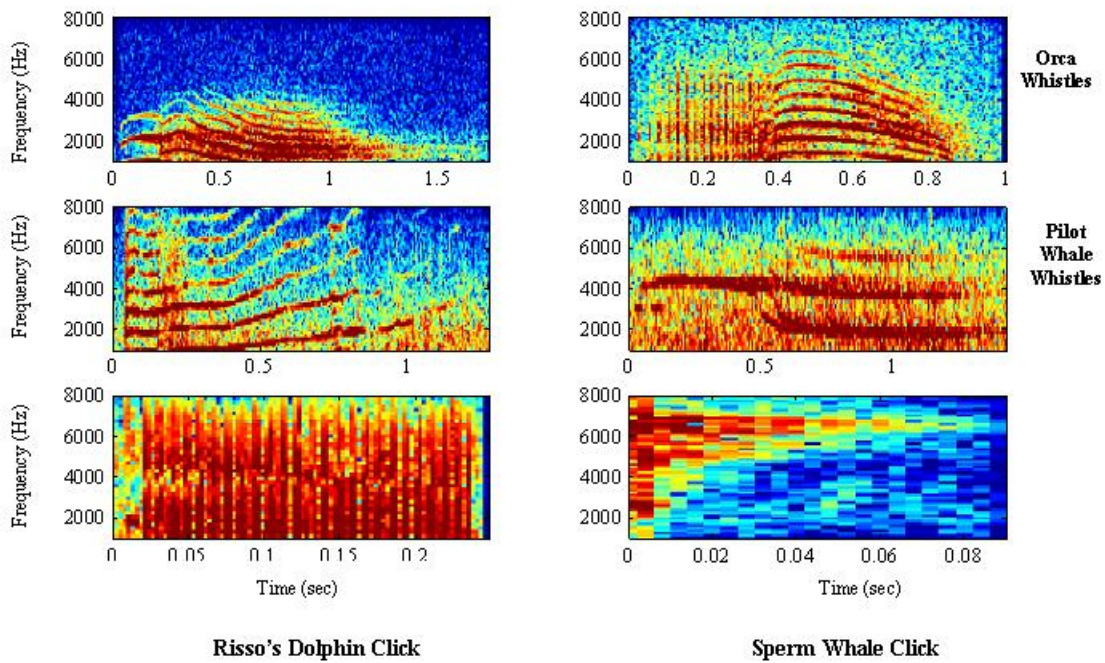


Figure 3: Spectrogram plots of frequency vs. time for the six selected whale calls. From left to right: (top row) orca1 and orca2 whistles, (middle) pilot1 and pilot2 whistles, (bottom) Risso's dolphin and sperm whale clicks.

C. ENVIRONMENTAL CONDITIONS AND BACKGROUND NOISE

CTD casts (conductivity/salinity, temperature, depth profiles) were conducted at the outermost and middle stations of each run. Little variation was seen in the sound velocity profiles measured over the course of the experiment (example shown in Fig. 4).

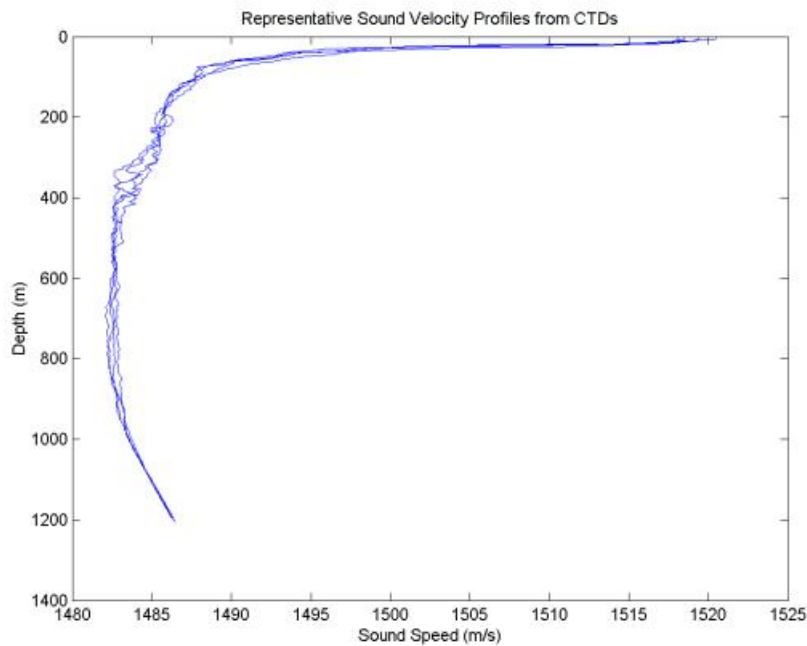


Figure 4: SCIUR sound speed profiles from 25-27 July 2002 (Rago, 2002).

Given the absence of a mixed layer and the presence of strong downward gradients near the surface of this profile, surface boundary layer interactions are minimal. In this situation, changing surface roughness characteristics due to variable wind conditions will not result in large variations of transmission loss between the source and receiver. Sea state and swell conditions were consistent throughout the data collection effort. Beaufort numbers of 3-4 were observed, corresponding to measured winds of 8-15 kts. Brief periods of winds less than 8 kts were also encountered, but extreme wind and swell events were not observed. Additional field studies or modeling simulations are required to characterize higher wind and sea state environmental effects upon Odontocete detection.

D. DATA ANALYSIS

The fifty transmissions of each whale call ensemble extended over multiple one-minute data acquisition files. End points were identified by locating 3 kHz marker tones between whale ensembles, then the targeted files were loaded, concatenated, interpolated to account for storage processing delays on the order of 0.1 seconds between data files, and trimmed to the ensemble duration. The resulting time series was converted from units of volts into Pascals (using an amplifier gain of 10 dB and SCIUR hydrophone sensitivity of -164.8 dB re $1 \text{ V}/\mu\text{Pa}$), then passed through an 8th order Butterworth filter with a passband from 1 to 8 kHz before being processed by the two detectors.

1. Matched Filter Detector

The matched filter detector was the first detector explored. This detector operates by comparing a replicant of the known transmitted whale signal to the received data. In this manner, incoherent noise is optimally reduced, making this the optimum detection method with a known source. The detector functions similarly to a cross-correlation function

$$C(m) = \sum_{n=1}^N W(m+n)R(n)\Delta t$$

where C is the detector output, R is the replicated reference signal, W is the received data, and Δt is the time increment (Medwin and Clay, 1998). An example of the matched filter performance is shown in Figure 5. In this case a whistle designated “orca2” is correlated against a filtered dataset containing the received multipath arrivals of the orca2 signal in a high SNR environment. The

detector output was partitioned based upon the known length of the broadcast whale signal, and the peak value within each window was recorded as a “hit” as shown in Figure 6.

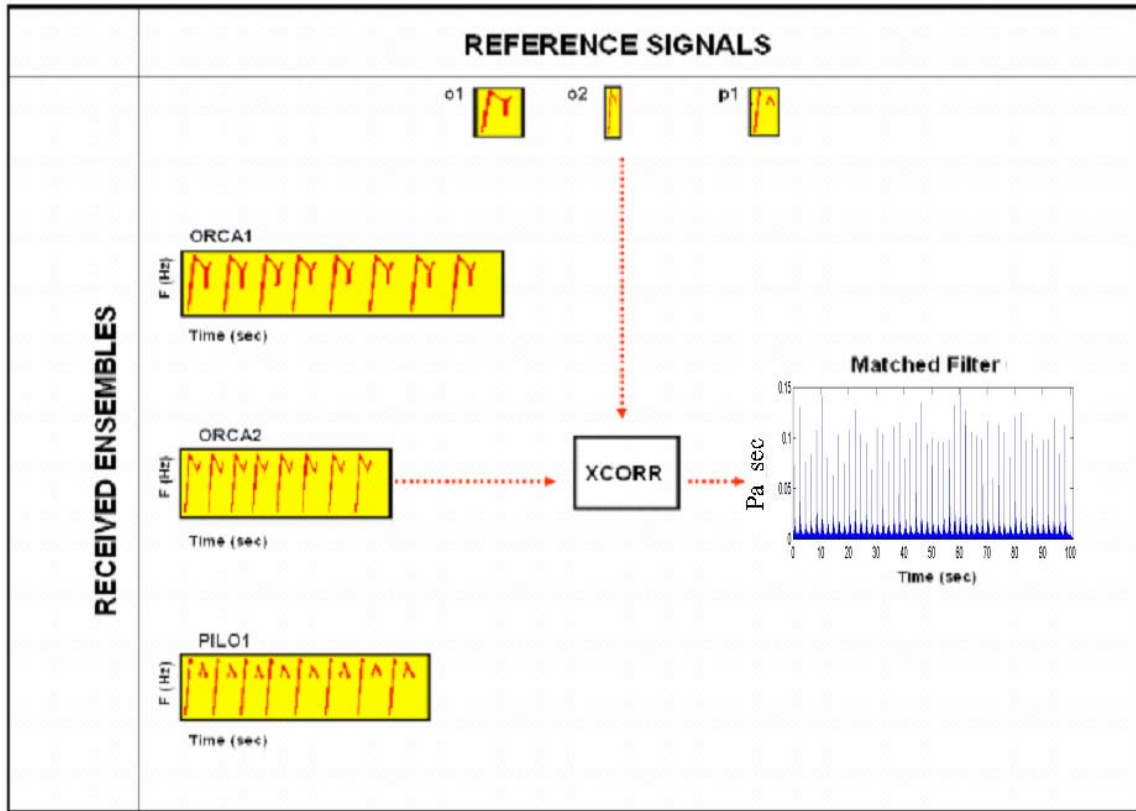


Figure 5: Operation of the matched filter detector (from Garcia, 2002). Transmitted time series of correlated whale ensembles are shown on the left as detector inputs, while the detector reference signals are shown at the top. The detector output for an orca2 whistle is shown on the right, with peak values indicating "hits" as described in Figure 6.

The targeted replicant signal was normalized prior to correlation with the received data. For a reference signal R of length N and time increment Δt , the normalization was:

$$\sum_{n=1}^N R^2(n)\Delta t = 1 \text{ sec}$$

with R being non-dimensional (unitless). The correlation feature of this detector can also be used to enable classification of the received whale signals. Varying the detector's reference signal against an ensemble time series will yield much lower resultant "hit" values if the replicant waveforms are significantly different.

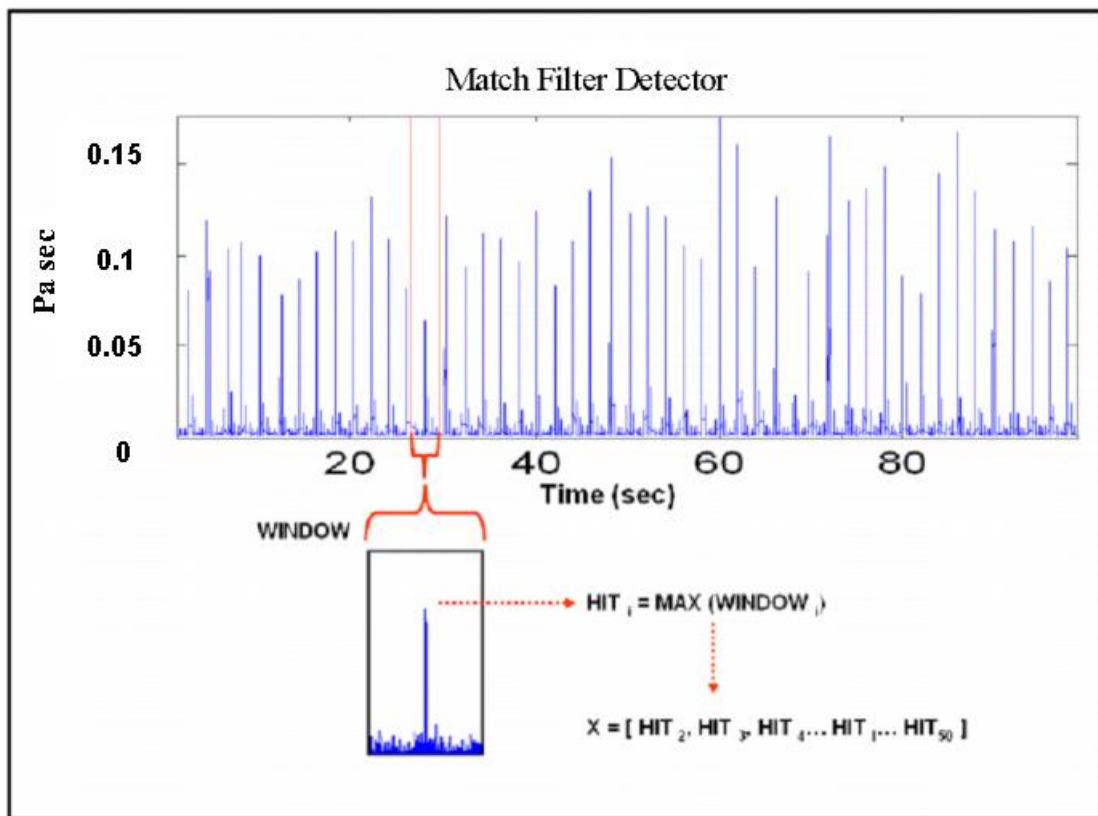


Figure 6: "Windowing" of the matched filter detector output (from Garcia, 2002). Peak values within each window were recorded as "hits" for detection probability statistics, and midpoints between hits were used to locate ambient noise samples within the received whale ensemble transmission to generate false alarm probability statistics.

2. Energy Detector

An energy detector was the second detection method explored. This is an incoherent detector, impartial to the waveform characteristics of the reference signal. It can be expressed as

$$C(m) = \sum_{n=1}^N W^2(m+n)U(n)\Delta t$$

where C is the detector output, W is the received data, Δt is the time increment, and U is a box function of unit amplitude and length $N\Delta t$, corresponding to the duration of the reference signal (Medwin and Clay, 1998).

The energy detector measures the total received energy and exploits the fact that signal is strongly correlated in time and noise is not. A strong, high-energy signal and incoherent noise field maximize detector performance. Detector “hits” are measured using the windowing scheme based upon the length of the known reference signal.

Since this detector does not rely upon the reference signal waveform characteristics, only its total energy, the energy detector is the optimal detector against an unknown source. In the presence of a discreet, coherent noise source, the performance of the energy detector degrades.

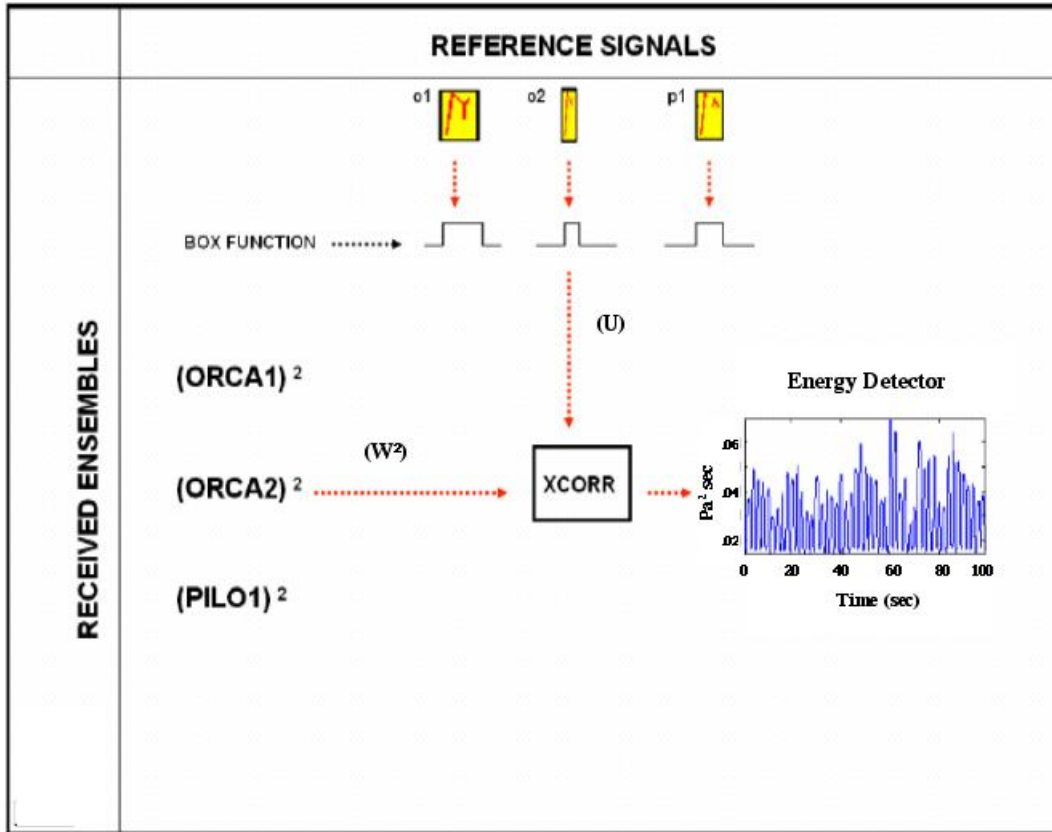


Figure 7: Operation of the energy detector (from Garcia, 2002). Transmitted time series of whale ensembles are shown on the left as detector inputs (W), while the unit amplitude box functions (U) that correspond to the reference signal durations are shown at the top. The detector output for an orca2 whistle is shown on the right.

3. Ambient Noise Analysis

Noise can be defined as any unwanted or undesirable sound, and is characterized in three ways: distributed or ambient noise, discrete interfering sources, and self noise from the equipment. Within the 1 to 8 kHz band, ambient noise (AN) is primarily caused by local wind forcing upon the sea surface (Tolstoy, 1993). This ambient noise level varies with changing wind speeds, as previously illustrated by Wenz (1962):

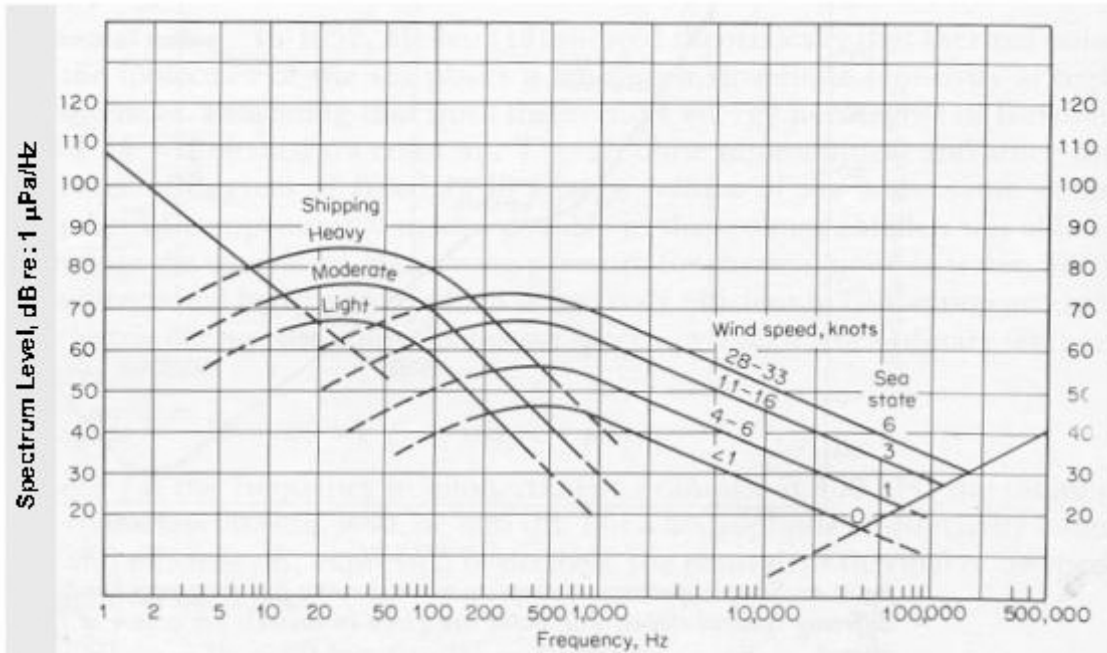


Figure 8: Average deep-water ambient-noise spectra (Urick, 1983).

Discrete noise sources created the largest variation in AN during this experiment. Transient marine mammals, active navy sonar, and fast boats were heard in the operating area during the data collection effort, raising the background noise levels and lowering the resultant SNR of the transmitted whale calls. Previous research concluded that the broadband noises generated by high speed zodiac motorboats can mask sperm whale clicks to distances exceeding 10 kilometers (Erbe, 2002).

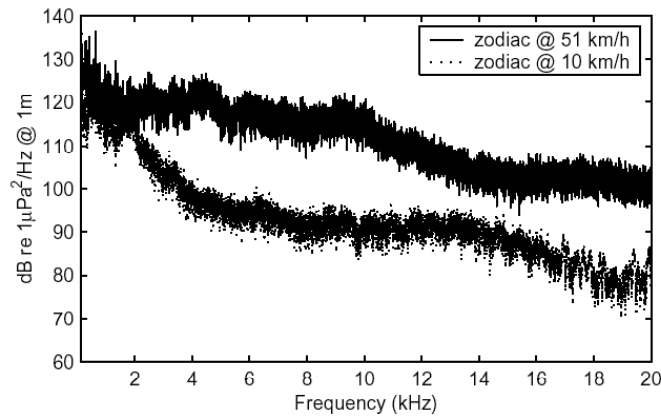


Figure 9: Power density spectra of slow and fast motorboats (Erbe, 2002).

Several hours of ambient noise data were collected, filtered, and demeaned to estimate the AN variance throughout the experiment. However, the unscheduled arrival and random duration of the discrete transient noise sources during the playback experiment precluded the use of these long-term mean estimates for AN levels. The transmission of one broadcast, fifty transmissions of all six whale calls, took nearly 15 minutes. Yet within one ensemble, fifty transmissions of only one call, the variance from discrete sources was evident as illustrated in Figures 10 and 11.

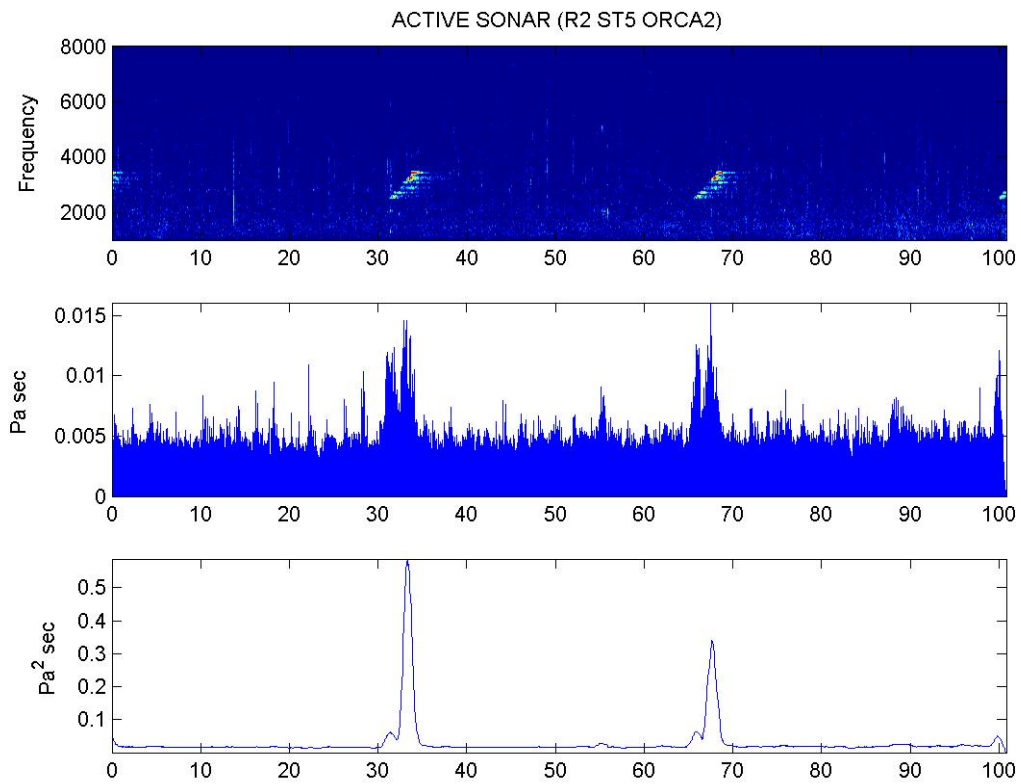


Figure 10: Ambient noise (AN) variability due to active Navy sonar transmissions during the broadcast of an orca2 whistle ensemble (50 repetitions). The discrete noises are visible in the spectrogram of the time series (top), matched filter output (middle), and the energy detector output (bottom).

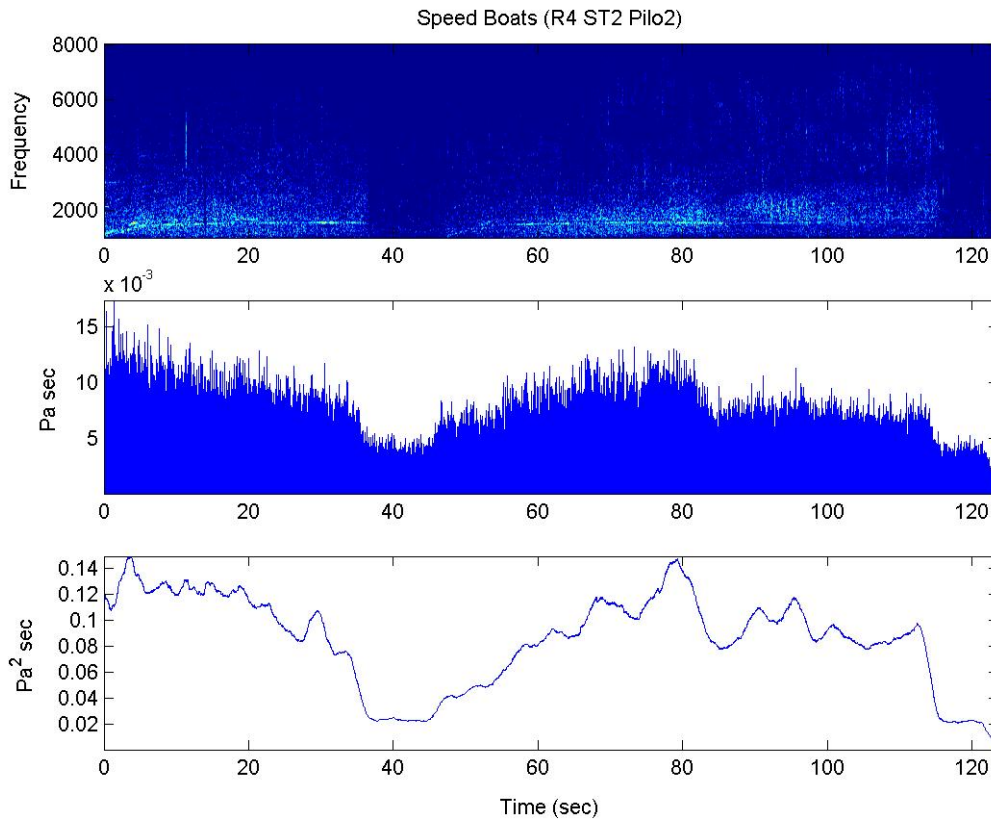


Figure 11: Ambient noise (AN) variability due to the operation of a high speed motor boat in the vicinity of the SCIUR vertical line array during transmission of a pilot2 whistle ensemble (50 repetitions). The discrete noise variability is visible in the spectrogram of the time series (top), matched filter output (middle), and the energy detector output (bottom).

To account for this variance, 0.2 second noise samples were taken from the one second pause between the individual signal transmissions. This sampling was done automatically by using the matched filter correlation detector to locate the midpoints between sequential signal “hits,” then extracting the noise segments from the original recorded data. Each noise sample was then replicated to match the duration of the six reference signals, and passed through the energy and matched filter detectors to generate the noise statistics for calculating the false alarm rates.

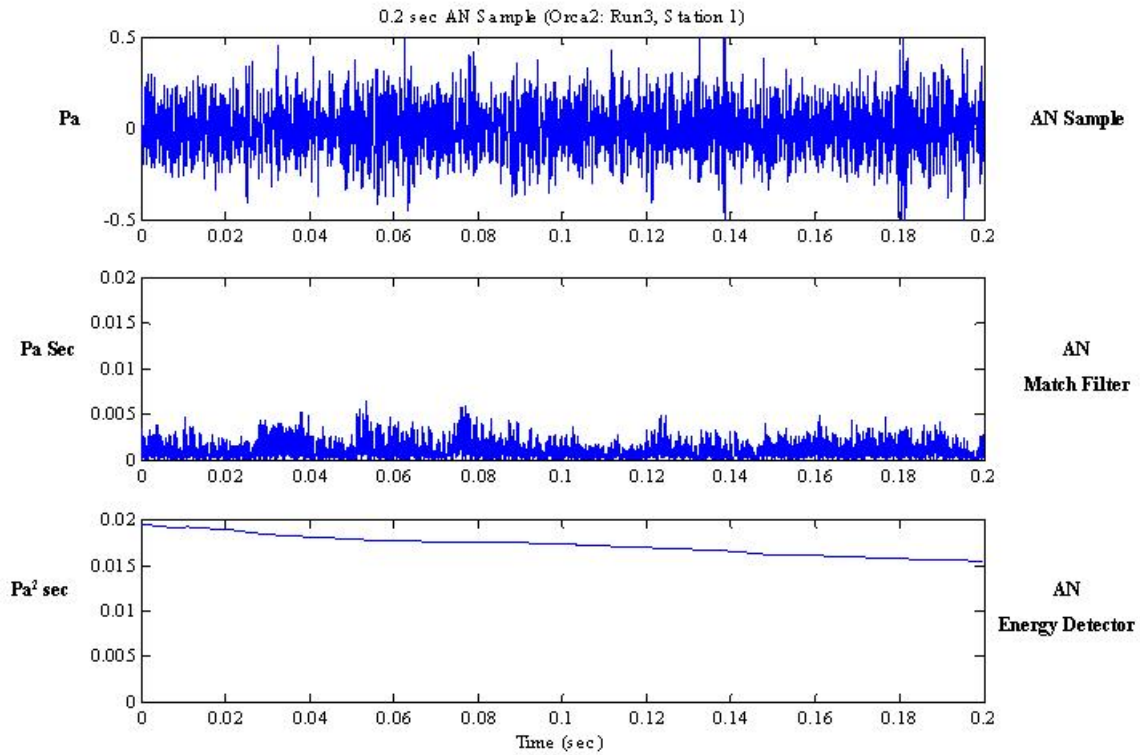


Figure 11: The top frame shows a 0.2 s ambient noise sample taken from the recorded SCIUR array data midway between subsequent orca2 whistle “signal hits” as identified by the matched filter detector (top). The sample was then replicated to match the duration of the reference signal, and passed through the matched filter (middle) and energy detectors (bottom) to generate noise “hits.”

4. Source Level Calculations

The source level (SL) for each whale call was determined from data collected by the calibrated monitoring hydrophone tethered astern the *R/V Pt. Sur*. Since the relative positions of the G34 transducer and monitoring hydrophone were not fixed, it was assumed the weight of the G34 would yield a near vertical position beneath the ship’s winch, while the position of the

lightweight hydrophone and 30 m of cable would vary dependent upon the relative current. The bounds of the source to monitoring receiver distances are shown in Figure 12:

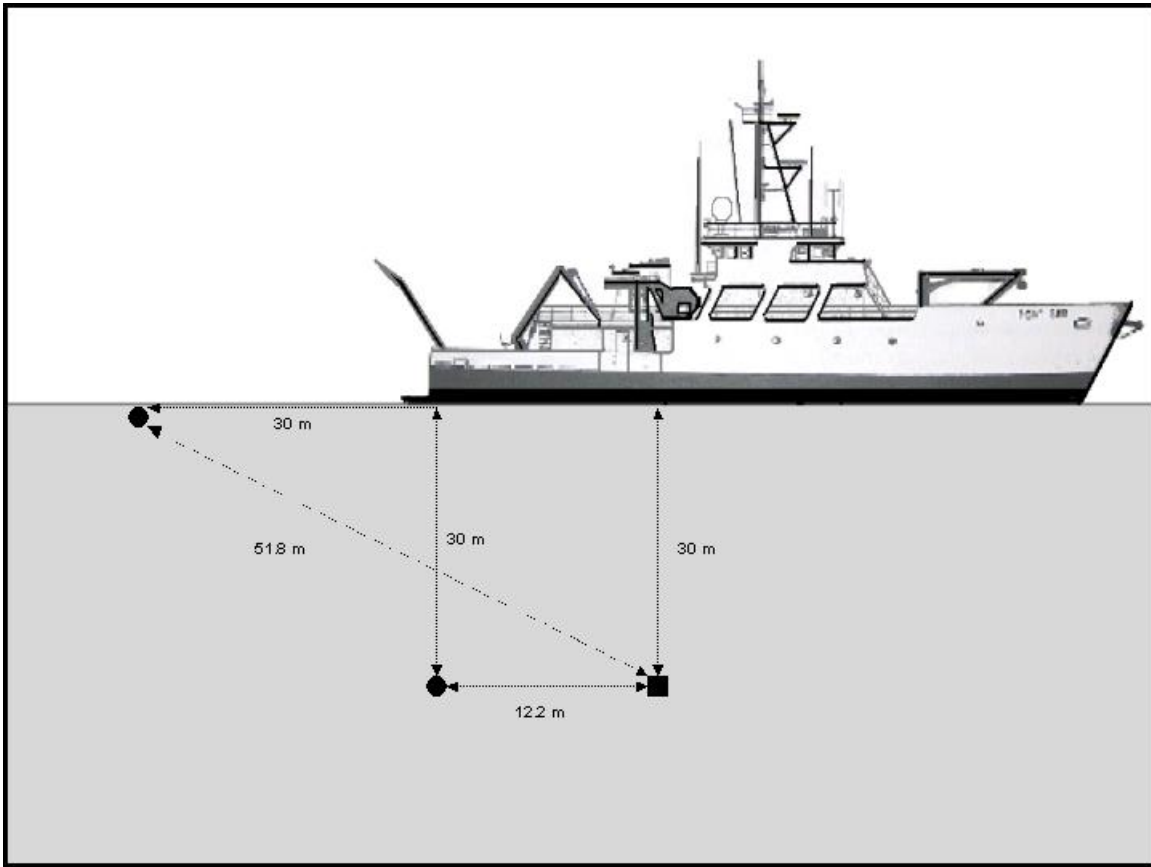


Figure 12: Relative positioning of the monitoring hydrophone to the vertical hanging G34 transducer. Ranges varied from 12.2 to 51.8 meters (Garcia, 2002).

As detailed by Garcia (2002), pressure values 1.0 m from the source were calculated by applying the receiver sensitivity (-164.8 dB re 1V/ μ Pa), amplifier gain correction (10 dB), and transmission loss removal for the upper and lower range limits to the measured data. In removing the transmission loss, spherical spreading was assumed.

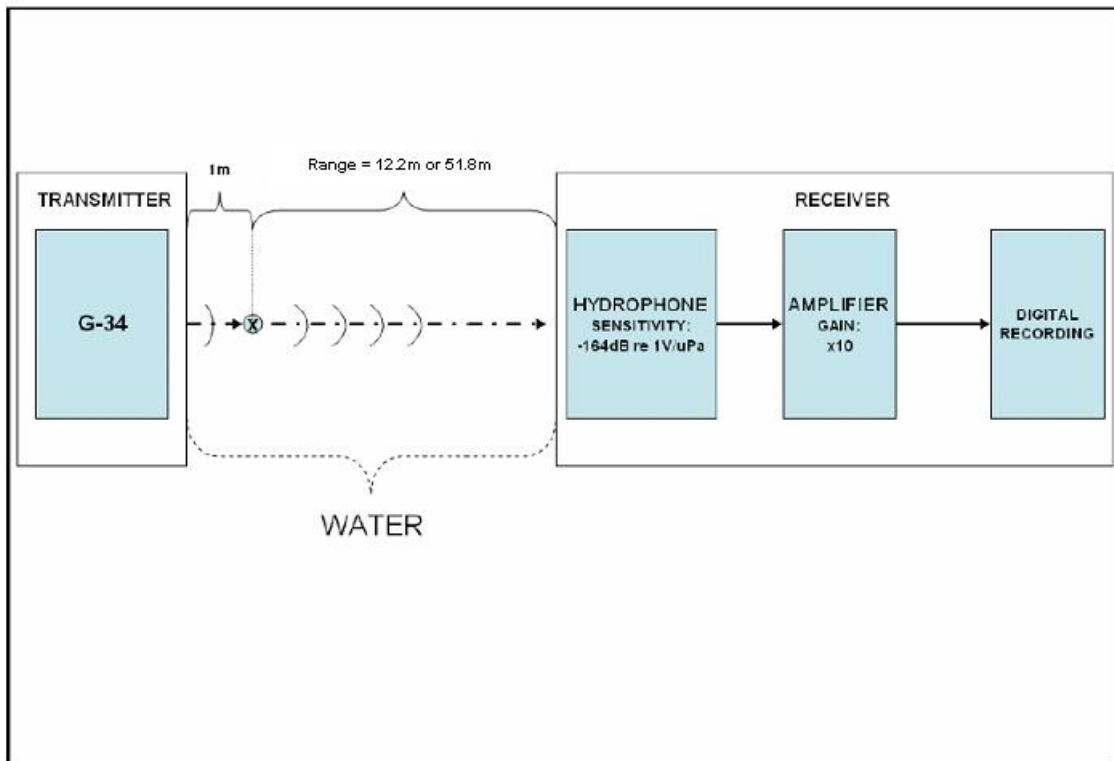


Figure 13: Diagram of system setup for source level (SL) computations, expressed in units of dB re 1 μPa @ 1 m (Garcia, 2002).

The SL was then computed as the mean squared pressure in the passband:

$$SL = 10 \log_{10} \left\{ \frac{\frac{1}{T} \int p_0^2(t) dt}{1 \mu\text{Pa}^2} \right\}$$

where T is the duration of the signal (seconds).

THIS PAGE INTENTIONALLY LEFT BLANK

III. RESULTS AND ANALYSIS

A. SOURCE LEVELS

Ensemble datasets for all five runs were sampled and averaged to determine mean source levels for each transmitted signal. Using the matched filter detector, the fifty whale signal repetitions within the sampled ensembles were located and extracted from the calibrated monitoring hydrophone data. The source level (SL) calculation results are shown in Table 1.

Whale Call	SL (12.2 m)	SL (51.8 m)	Cited SL
Orca1	139.1	145.3	178.0
Orca2	141.9	148.2	178.0
Pilot1	141.3	147.6	178.0
Pilot2	140.3	146.6	178.0
Risso	138.0	144.3	175.0
Sperm	138.5	144.8	232.0

Table 1: SL calculations for the six selected whale signals, computed for both 12.2 m and 51.8 m source to receiver path ranges. The last column lists source levels cited in current literature. Units are dB re 1 μ Pa measured at 1.0 m from source (Richardson, et al., 1995 and Ocean Noise and Marine Mammals, 2003).

Differing source levels were expected given the variations in signal waveforms. The two shortest duration signals (Risso's dolphin and sperm whale clicks) had the lowest observed SL during the playback transmissions. Hardware constraints limited all source levels generated during this experiment significantly below the values cited in current literature as indicated in Table 1 (Richardson. et al., 1995; Au, 1993; and Ocean Noise and Marine Mammals, 2003).

B. CURVE FITTING

Smooth probability density functions (PDFs) were generated by fitting continuous functions to the measured histograms of the hits. Gamma and normal distributions were compared to normalized histograms of the matched filter and energy detector outputs using a Kolmogorov-Smirnov goodness-of-fit test.

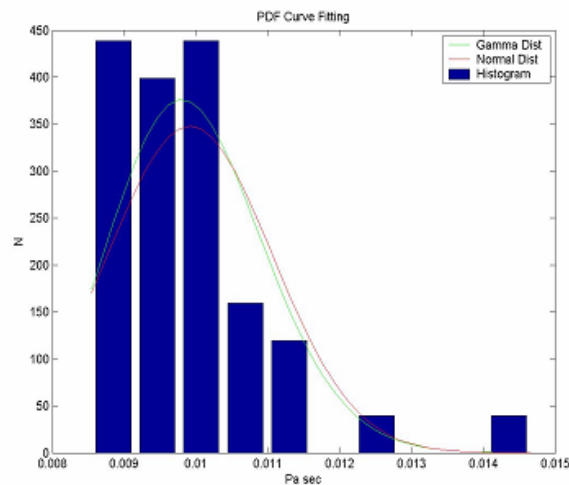


Figure 14: Normalized histogram of orca1 whistle matched filter “hits” in the presence of signal, fitted with normal and gamma distributions.

The adequacy of the fits for the detector histograms of the signal (hits in the presence of signal) and noise (hits when signal was absent) from all runs, stations, and channels was tallied for each whale call. These tests verified the preliminary results observed by Garcia (2002): (1) the gamma distribution had the least rejections and was therefore the best fit; (2) the matched filter output was more closely represented than the energy detector by the gamma distribution; (3) and the presence of discreet, transient signals caused deviations of the observed histograms from the gamma probability density functions. The effects of the discrete noises were most apparent upon the energy detector, and

caused an order of magnitude shift in the detector's output when an active navy sonar and high speed boat traffic were operating in the vicinity. The correlation capability of the matched filter was degraded less by these coherent noise sources, and yielded better detector performance in the low SNR conditions.

The signal and noise probability density functions were then reproduced using a gamma distribution:

$$y = f(x | a, b) = \frac{1}{b^a \Gamma(a)} x^{a-1} e^{-\frac{x}{b}},$$

where the gamma function (Γ) was defined by the integral:

$$\Gamma(a) = \int_0^{\infty} e^{-t} t^{a-1} dt$$

and the gamma distribution shaping parameters a, b were computed from the normalized histogram mean (\bar{x}) and variance (s^2):

$$a = \frac{\bar{x}^2}{s^2} \quad \text{and} \quad b = \frac{s^2}{\bar{x}}$$

In order to generate the gamma distributions at any point along the transmission path, the mean and variance of the hits (x) in the matched filter and energy detector output for each of the source signals were plotted against range as recorded by GPS. Ensembles from all runs, stations, and channels were plotted after the elimination of the extreme transient noise events. No depth dependence of the plotted data points was evident to visual inspection. All data points were therefore concatenated and fitted using the relationship:

$$Y_N = g(X-X_0)^n$$

where Y_N = resultant magnitude of the mean and variance, X is the horizontal range, X_0 is the minimum measured range, and n is a decay parameter (negative power).

The ambient noise data was fitted using the mean. The more conservative approach of estimating AN by the maximum observed noise level was not feasible for this dataset. Ambient noise levels measured while transmitting whale signals at stations under three kilometers from the SCIUR array were higher due to self-noise generated by the *R/V Pt Sur*. The noise maxima observed when the ship was further from the array were indicative of discreet, transient sources, and not representative of an overall fluctuation in the environmental conditions or shipping levels within the area. The mean of noise values measured during each whale signal ensemble broadcast of fifty repetitions was therefore deemed an appropriate estimate of the prevailing AN.

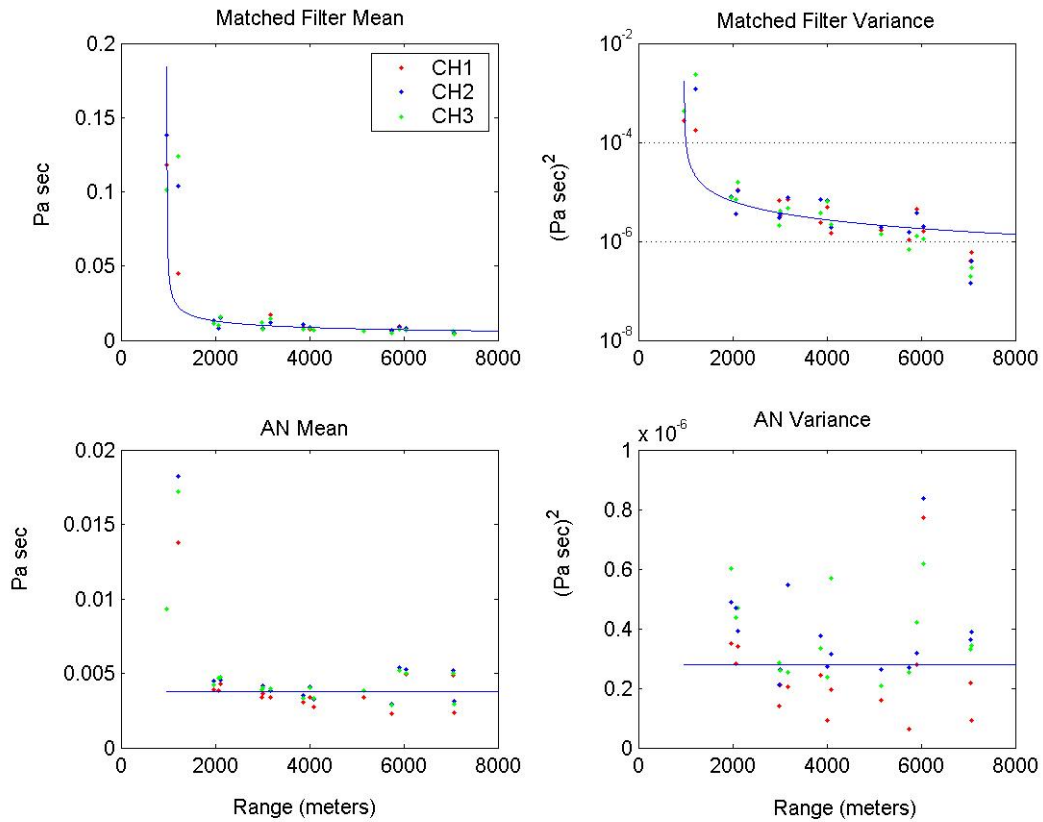


Figure 15: Curve fitting of the matched filter detector outputs for the orca1 whistle received by transducers at 75.3 m (CH 1), 136.6 m (CH 2), and 165.8 m (CH 3) depths. The signal mean and variance points are shown above together with the best fit curve, while the acoustic noise (AN) points were fitted by mean values as shown below.

Using the mean (\bar{x}) and variance (s^2) values from the fitted curves as illustrated in Figure 15 for the case of the orca1 whistle, the gamma distribution shaping parameters a , b could then be calculated at any point along the transmission path to generate the “signal” and “noise” gamma distributions as shown in Figure 16.

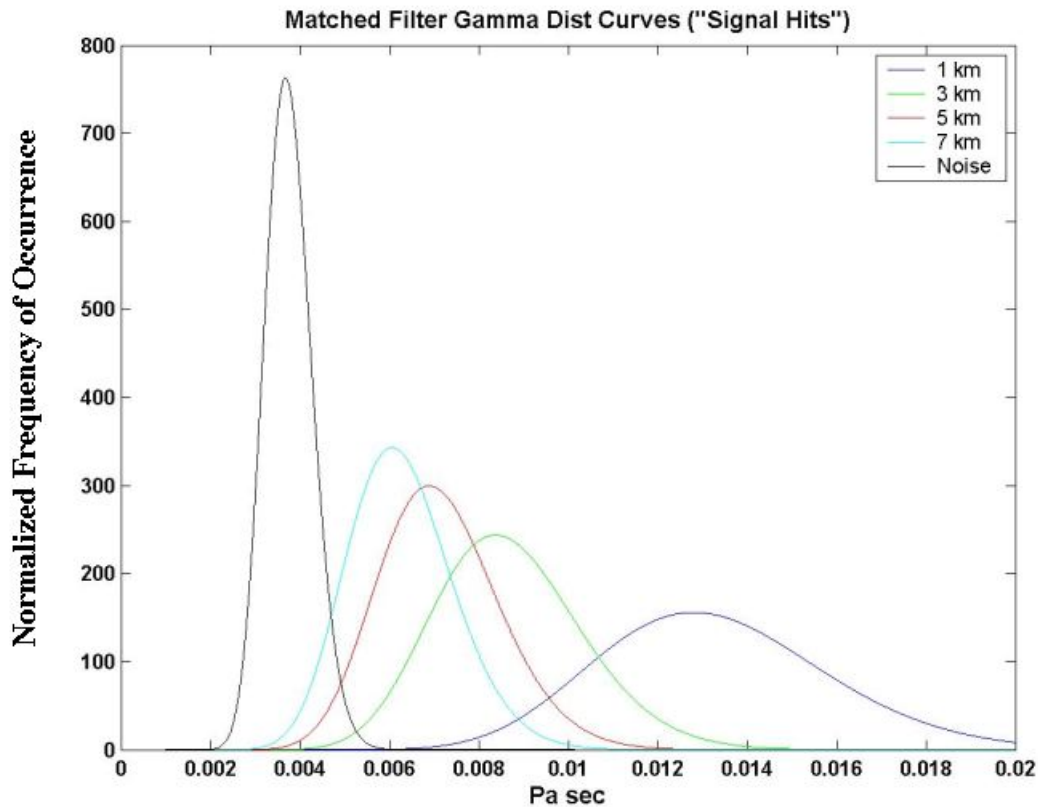


Figure 16: Gamma distributions used to represent PDFs of the matched filter detector outputs (hits) for the orca1 whistle, interpolated from the best-fit mean and variance curves. Distributions of detector output peaks in the presence and absence of a whale signal (labeled as 1 to 7 km distances and "noise" respectively) are shown.

C. DETECTOR PERFORMANCE CURVES

The probabilities of detection for given false alarm rates were plotted against range and signal to noise ratio (SNR) to develop the receiver operating characteristics (ROC) curves. SNR is the ratio of the received signal energy and noise energy, prior to the addition of processor gains such as from the matched filter detector. The peak value in each energy detector "signal" window was actually a measure of signal energy plus noise energy, or (S+N). Noise values (N) were obtained by passing replicated ambient noise samples, trimmed to the

reference signal duration, through the energy detector and sampling the peak values using the windowing process. The mean of the energy detector signal and noise were then used to solve for SNR:

$$SNR = \frac{(S + N) - (N)}{(N)}$$

This is the linear SNR ratio. $10 \cdot \log$ of this linear ratio yields the SNR in decibels.

Both the matched filter and energy detector outputs for all six whale signals and noise estimates were plotted and analyzed. By definition, the false alarm rate, $P(FA)$, is the area under the detector output PDF when signal is absent that lies to the right of a given threshold. The probability of detection, $P(D)$, is the area under the detector output PDF with signal present that lies to the right of the threshold.

1. Matched Filter and Energy Detector Performance

To facilitate the comparisons of the performance curves for different whale calls, the 90% and 50% probabilities of detection with false alarm rates fixed at 1% were selected for discussion. These represent a high probability of detection situation ($P(D)$ of 90% and $P(FA)$ of 1%), and a minimum acceptable detection situation ($P(D)$ of 50% and $P(FA)$ of 1%). Using these criteria, the energy and matched filter detectors' performance was gauged using the SNR and range limits of detection (given the measured SL of approximately 140 dB re 1 μ Pa) for each whale call.

a. Orca1 Whistle

The first orca whistle, designated orca1, demonstrated a 90% probability of detection with a 1% false alarm rate at -7 dB SNR for the matched filter. For the project's 140 dB re $1 \mu\text{PA}$ source level, the high detection/low false alarm rate case realized detection ranges of approximately 1500 m. This same detector achieved the 50% P(D), 1% P(FA) at -8 dB, or 3000 m for the measured SL.

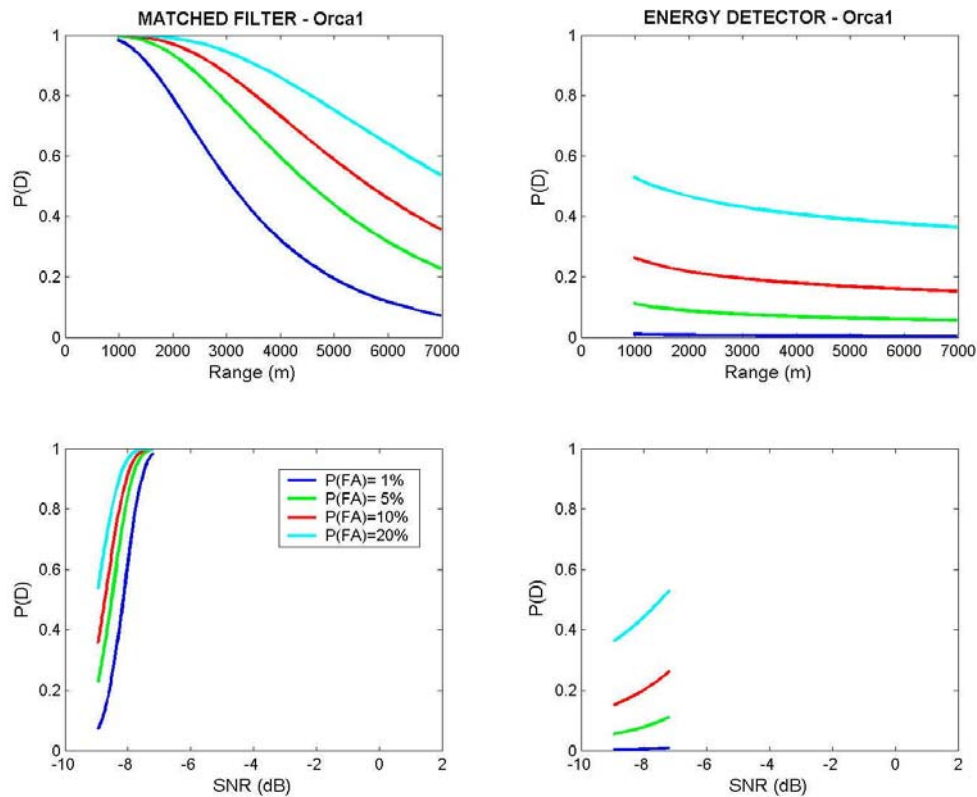


Figure 17: Receiver operating characteristics (ROC) curves for the orca1 whistle. Matched filter detector (left) and energy detector (right), with P(D) vs. range (top) and P(D) vs. SNR (bottom) for both. For the range of SNR realized in this playback, the largest P(D) achieved by the energy detector was 0.55 with a P(FA) = 20%.

The energy detector performance was significantly worse than the matched filter in detecting the orca1 whistle. For the range of SNR values realized in the playback of this signal, which were all less than -7 dB, the energy detector never achieved the 1% P(FA), and only at 20% P(FA) was a P(D) greater than 50% observed.

b. Orca2 Whistle

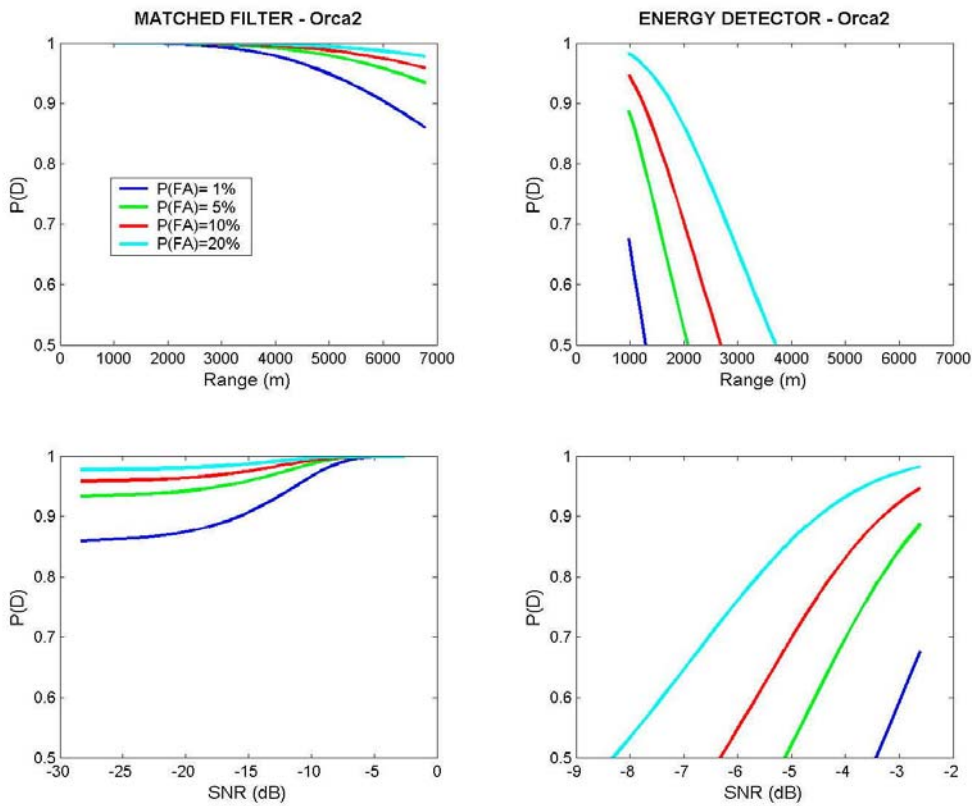


Figure 18: Receiver operating characteristics (ROC) curves for the orca2 whistle. Matched filter detector (left) and energy detector (right), with P(D) vs. range (top) and P(D) vs. SNR (bottom) for both.

The orca2 whistle maintained above 90% P(D) 1% P(FA) through -16 dB SNR for the matched filter detector (corresponding to 6000 m for the SL of 140 dB re 1 μ PA). At the minimum realized SNR of approximately -28 dB, the

P(FA) of 1% still had a P(D) of 85%; the lower limit of 50% P(D) was not realized with the 1% false alarm rate within this range of SNR values. The energy detector had a P(D) of 65% for the 1% P(FA) at the maximum observed SNR of approximately -2.5 dB. The 50% P(D) was reached at -3.5 dB SNR for the same P(FA). The energy detector range limit for detection in both these instances was 1000 m for a 140 dB re 1 μ PA SL.

c. Pilot1 Whistle

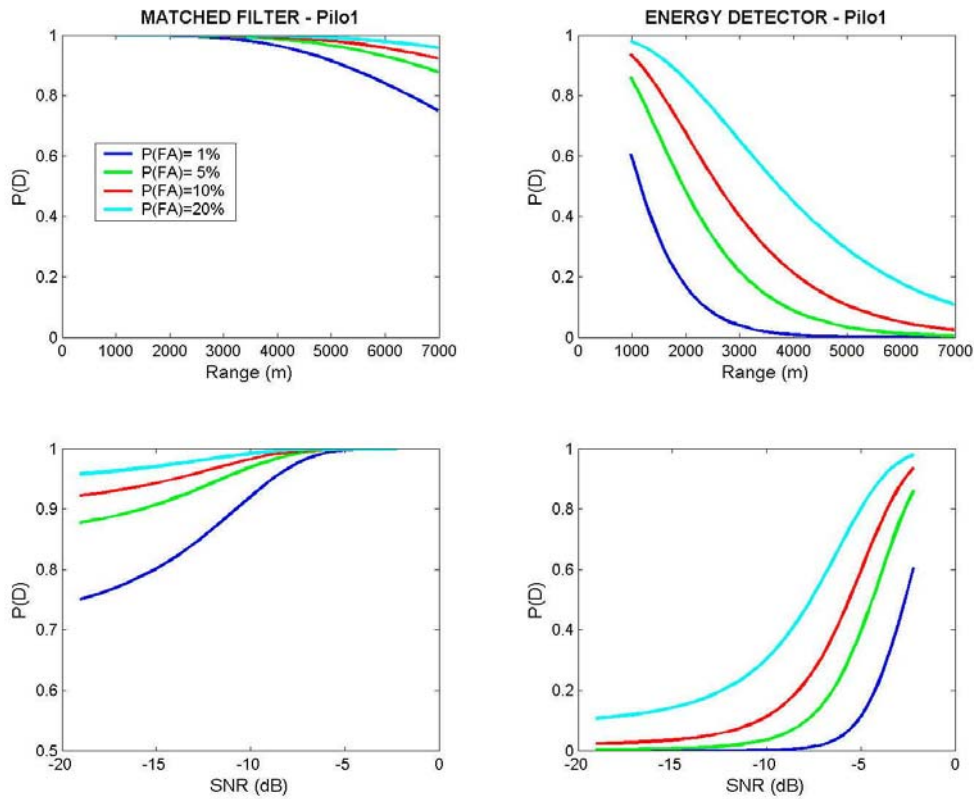


Figure 19: Receiver operating characteristics (ROC) curves for the pilot1 whistle. Matched filter detector (left) and energy detector (right), with P(D) vs. range (top) and P(D) vs. SNR (bottom) for both.

The pilot1 whistle matched filter detector had a 90% or greater P(D) for the P(FA) of 1% through -10 dB SNR (or 5000 m for the 140 dB re 1 μ PA

SL). This detector yielded a 75% P(D) at -18 dB for the 1% P(FA), corresponding to a 7 km detection range for the 140 dB re 1 μ PA SL. The energy detector achieved a maximum of 60% P(D) with a 1% P(FA) for the realized -2 to -8 dB SNR range, and a detection range of just over 1000 m at the 50% P(D) level for the 1% P(FA) and source level of 140 dB re 1 μ PA.

d. Pilot2 Whistle

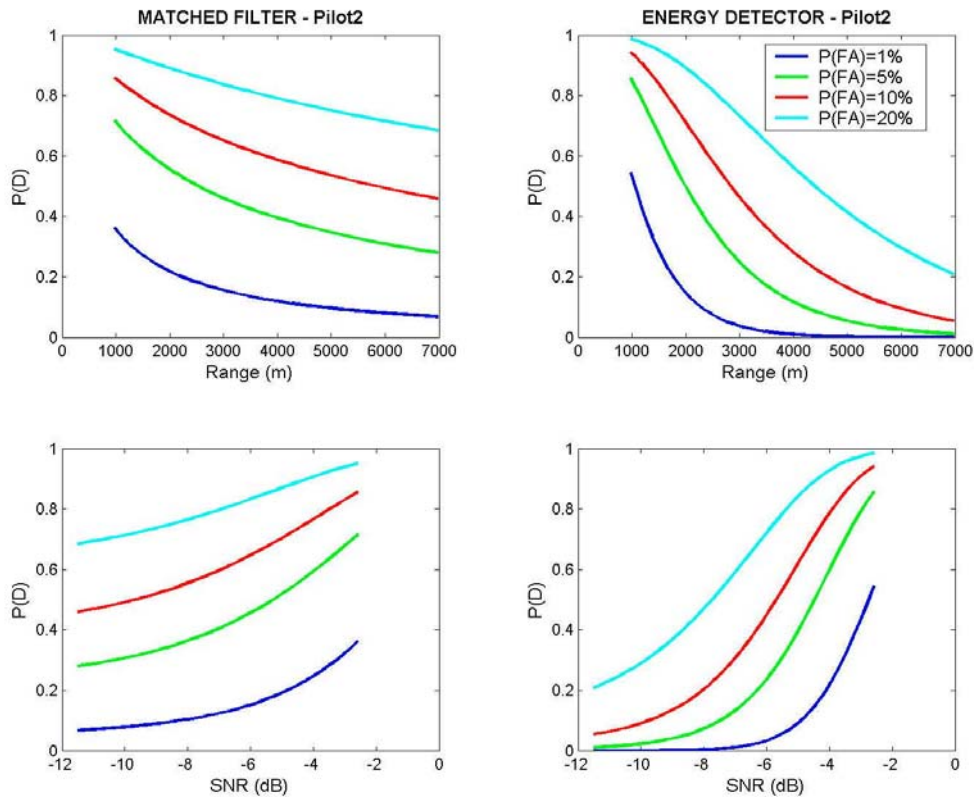


Figure 20: Receiver operating characteristics (ROC) curves for the pilot2 whistle. Matched filter detector (left) and energy detector (right), with P(D) vs. range (top) and P(D) vs. SNR (bottom) for both. For the range of SNR realized in this playback, the highest observed P(D) was 73% for a 5% P(FA), corresponding to an SNR of -2.5 dB and range of approximately 1000 m for the 140 dB re: 1 μ PA source level.

The matched filter detector did not yield above a 50% detection probability for the P(FA) of 1% when analyzing the pilot2 whistle. The 1% P(FA)

did exceed 50% $P(D)$ for this pilot whistle using the energy detector, achieving a 55% $P(D)$ at -3 dB SNR and detection range of 1 km for the 140 dB re $1 \mu\text{PA}$ source level.

e. *Risso's Dolphin Click*

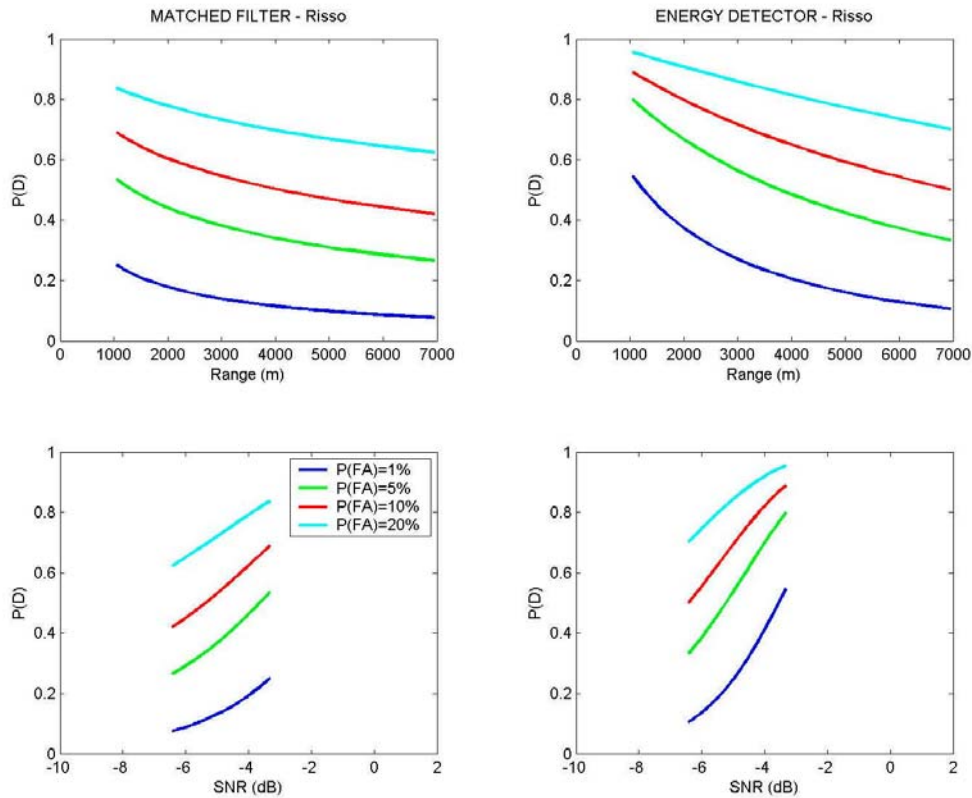


Figure 21: Receiver operating characteristics (ROC) curves for the Risso's dolphin click. Matched filter detector (left) and energy detector (right), with $P(D)$ vs. range (top) and $P(D)$ vs. SNR (bottom) for both. For the range of SNR realized in this playback, the $P(D)$ for the 1% $P(FA)$ did not exceed 50%. A 55% $P(D)$ was observed for the 5% $P(FA)$.

For the -3 to -7 dB SNR range realized during the playback of the Risso's dolphin click, the highest observed matched filter detection probability did not exceed 50% for the 1% false alarm rate. The energy detector achieved a maximum of 55% $P(D)$ with a 1% $P(FA)$ at -3 dB SNR. A detection range of

1200 m was realized by the energy detector for the 50% P(D) and 1% P(FA) situation (source level of 140 dB re 1 μ PA).

f. Sperm Whale Click

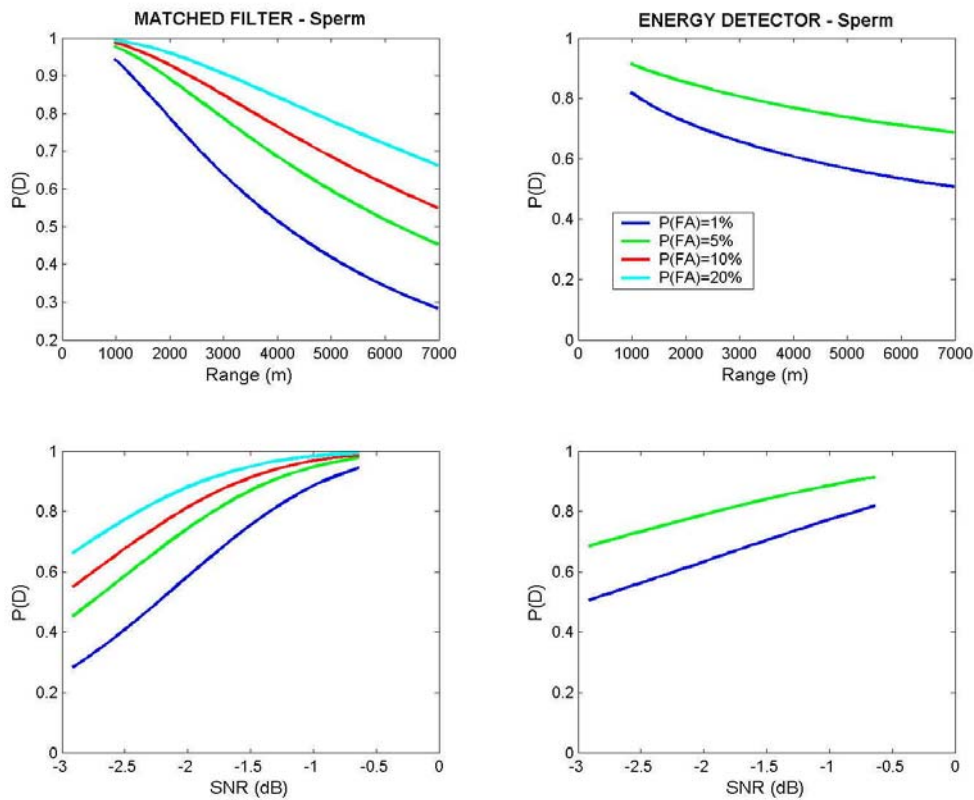


Figure 22: Receiver operating characteristics (ROC) curves for the sperm whale click. Matched filter detector (left) and energy detector (right), with P(D) vs. range (top) and P(D) vs. SNR (bottom) for both.

Sperm whale clicks received above -1 dB SNR were detected 90% of the time by the matched filter at approximately 1500 m for the P(FA) of 1% and 140 dB re: 1 μ PA source level.. The 50% P(D) was realized at approximately -2

dB SNR, or at a range slightly greater than 4000 m for a SL of 140 dB re 1 μ PA with a 1% P(FA).

For the energy detector, the 1% P(FA) exceeded 80% P(D) at -1 dB SNR, yielding an observed detection range of approximately 1 km for the 140 dB re 1 μ PA source level. The 50% P(D) was realized at -3 dB SNR, at a detection range exceeding 7000 m, for a SL of 140 dB re 1 μ PA with a 1% P(FA).

2. Comparison of Detector Performance

Maximum Range (m) and Required Minimum SNR (dB) vs. P(D)			
	Match Filter P(D) = 90%	Matched Filter P(D) = 50%	Energy Det P(D) = 50%
Orca1	-7 dB 1500 m	-8 dB 3000 m	> 2 dB < 1000 m
Orca2	-16 dB 6000 m	< -28 dB > 7000 m	-3.5 dB 1000 m
Pilot1	-10 dB 5000 m	-18 dB 7000 m	-2.5 dB 1000 m
Pilot2	> -2 dB < 1000 m	> -2 dB < 1000 m	-3.25 dB 1000 m
Risso's Dolphin	> 2 dB < 1000 m	> 2 dB < 1000 m	-3.5 dB 1300 m
Sperm	-1 dB 1500 m	-2 dB 4000 m	-3 dB 7000 m

Table 2: Probability of Detection (P(D)) vs. range (meters) and signal to noise ratio (dB) for all six whale calls with a set false alarm rate of 1%. Summarized are the performance characteristics for the matched filter at 90% and 50% P(D), and energy detector at 50% P(D) values. For the energy detector, P(D) of 90% and higher were not observed for the SNR values realized in the playbacks. Range values are based upon a source level of 140 dB re 1 μ PA, and would vary with changes to source level.

Overall the matched filter detector outperformed the energy detector in the detection of a known signal. As shown in Table 2, the orca2 and pilot1 whistle matched filter detectors realized 5000 m detection ranges for the 90% P(D) and

1% P(FA) case, and 7000 m detection ranges for the 50% P(D) and 1% P(FA) case (SL = 140 dB re 1 μ PA). The orca2 whistle was detectable down to very low SNR: -16 dB for the 50% P(D) and below -28 dB SNR for the 90% P(D) (with a 1% P(FA) for both).

The good performance of the orca2 and pilot1 whistles was not shared by all signals. The other four signal results were two tiered: the orca1 whistle and sperm whale click had an order of magnitude lower SNR than the orca2 and pilot1 realizations, and the pilot2 whistle and Risso's dolphin click were unusable. The sperm whale click and orca1 whistle had detection ranges of 1500 m at the 90% P(D), 1% P(FA) with the 140 dB re 1 μ PA source levels, corresponding to a -1 dB and -7 dB SNR respectively. The sperm whale was observed at a greater range (4000 m) than the orca1 whistle (3000 m) in the 50% probability of detection example (P(FA) of 1% and 140 dB re 1 μ PA SL). The Risso's dolphin click and pilot2 whistle were not detectable with the matched filter at the 1% false alarm rate for the range of SNR realized during this playback.

The energy detector had mixed results too. The detector was unusable for the orca1 whistle detection, and normally demonstrated a 50-65% detection probability for the 1% false alarm rate between -2 to -3 dB SNR. The ranges of detection (given the SL of 140 dB re 1 μ PA) were approximately 1000 m. The energy detector demonstrated the highest performance with the sperm whale signal, achieving an 80% detection probability (-1 SNR, 1500m), and the largest detection range of all signals at 7000 m for the 1% P(FA), 50% P(D) situation, given the source level of 140 dB re 1 μ PA.

D. SIGNAL CLASSIFICATION

A preliminary analysis of signal classification was performed using the matched filter. Since the observed SNRs varied for all six signals, the direct

comparison of the matched filter's classification performance for the various whale calls was not possible.

The matched filter detector correlated the observed time series against the six selected whale signals transmitted during the experiment. Ensembles of each whale signal were filtered using an 8th order Butterworth filter, bandpassed from 1 to 8 kHz, then correlated against all six normalized and filtered reference signals. Both orca whistles, the pilot1 whale whistle, and the sperm whale click reference signals displayed strong classification tendencies, producing at least an order of magnitude higher filter outputs with the directly correlated data series than with the cross-correlated data (see Figure 23 for orca2 whistle example).

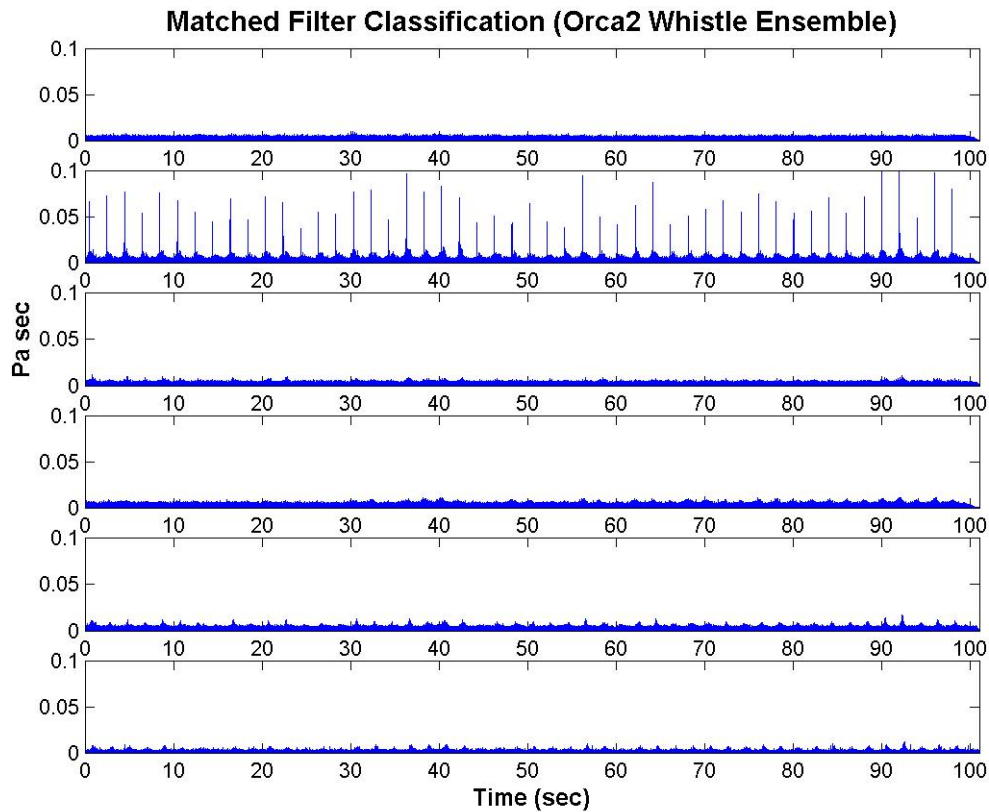


Figure 23: Matched filter classification performance for the orca2 whistle. From top to bottom, the correlation of an ensemble of orca2 whistle transmissions as referenced to the orca1, orca2, pilot1, pilot2, Risso's dolphin, and sperm whale signals.

The pilot2 whale whistle and the Risso's dolphin click did not provide strong classification capabilities, and exhibited direct-correlation and cross correlation matched filter results of approximately the same amplitude (see Figure 24 for Risso's dolphin example). The detectors' inability to strongly identify the signal waveforms precluded effective classification for these two cases.

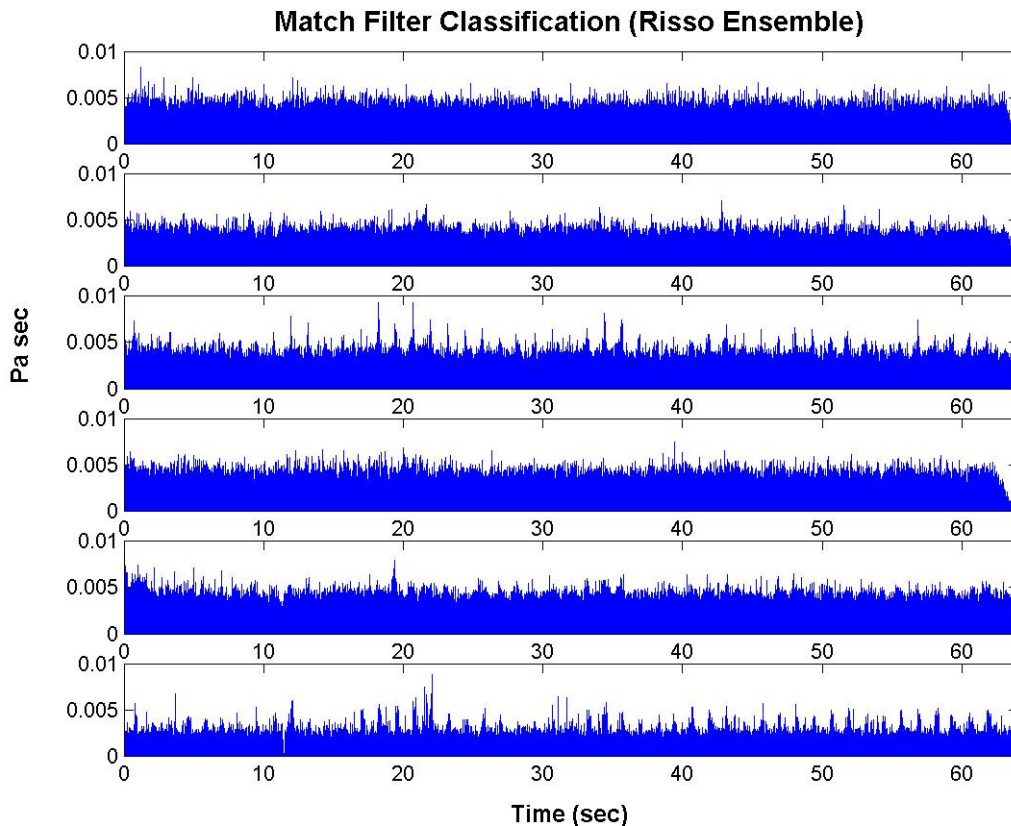


Figure 24: Matched filter classification performance for the Risso's dolphin click. From top to bottom, the correlation of an ensemble of Risso's dolphin clicks as referenced to the orca1, orca2, pilot1, pilot2, Risso's dolphin, and sperm whale signals.

No false correlations occurred from cross correlations between the whistles and clicks. Also no false positives were inherent when comparing a whistle ensemble to another whistle reference signal, or likewise when cross correlating the two replicated clicks. Even within the same species, such as orca1 vs. orca2 or the pilot1 vs. pilot2 whistles, the cross correlation values were

an order of magnitude lower than the direct correlations. These results indicate that a single recorded whistle or click sample is not suitable for species identification. For proper species identification, the classification library must contain an array of calls for each species.

IV. CONCLUSIONS

Playback experiments were used to quantify the performance of omnidirectional receivers for the passive acoustic detection of Odontocete vocalizations. Results provided comparative statistics for the probabilities of detection, false alarm rates, and detectable SNR and range limits for the signal source levels of approximately 140 dB re 1 μ Pa.

Based upon these results, the matched filter detector outperformed the energy detector for given probabilities of detection, false alarm rates, and SNRs against a known signal. Though two signals were not detected, the orca2 and pilot1 whistles exceeded 5000 m detection ranges for the probability of detection (PD) of 90% and false alarm rate (P(FA)) of 1% with the SL of 140 dB re 1 μ Pa. The energy detector had no P(D) above 90% at the 1% P(FA) for the range of SNR realized in this playback experiment, but all signals except the orca1 whistle were detectable beyond 1000 m with a 50% P(D) and the same P(FA). The sperm whale yielded the best energy detector performance, with detection ranges exceeding 7000 m for the 50% P(D), 1% P(FA), and source level of 140 dB re 1 μ Pa.

The Risso's dolphin click matched filter detector output had lower SNR values than the energy detector for comparative P(D) and P(FA), and also demonstrated weak correlation abilities for the classification analysis. This indicated that either correlated noise remained in the received signal after filtering, or that the reference signal did not contain prominent features for the matched filter correlation. Likewise the lower performance standards of the orca1 whistle compared to the orca2 signal were likely due to residual noise after filtering. Orca1 was the narrowest signal broadcast during this experiment, with little of the waveform exceeding 4 kHz (see Figure 3). Therefore, the frequencies between 4 and 8 kHz were noise and subsequently lowered the SNR. Future analysis or operational use should adopt a variable filtering scheme that matches the signals targeted for detection or classification.

Determination of detection distances from SNR values requires accurate knowledge of the targeted marine mammal source level. Given known environmental conditions and the target's SL, the source to receiver distance can be obtained from transmission loss calculations. Integrated measures of the total SL power are needed to characterize the whale call, not merely peak-peak amplitude values. The matched filter and energy detectors used in this experiment function by integration of the received signals, not by direct comparisons to the peak power values. The mean squared pressure (or power) source level measurements are necessary to compare different source signal levels, analyze detector performances, and validate detector classification capabilities.

The matched filter demonstrated great potential for classifying Odontocete signals. Further studies should focus upon the classification performance, ensuring equal SNRs for all replicated whale signals to permit the direct comparison of measured results. Predictive modeling also is needed to fill in gaps from field measurements, and extrapolate the performance results to different environmental conditions. Different wind regimes, sea states, bottom types and bathymetry, and shipping and biological ambient noises can all be examined by numerical models.

LIST OF REFERENCES

- Au, Whitlow W.L. The Sonar of Dolphins. New York, NY: Springer-Verlag, 1993.
- Borsani, J.F., S.S. Flayes, A. Molinari, and D. Costa. "Multiple Sperm Whales Tracked by Combining a Towed Dipole Hydrophone and Free-Drifting Spar-Buoy Arrays." [<http://home.snafu.de/ulisses/analysis/abstract.htm>]. Mar 2003.
- Chiu, Ching-Sang and James H. Miller. "Localization of the sources of short duration acoustic signals." Journal Acoustic Society of America 92 (November 1992): 2997-2999.
- Erbe, Christine. "Underwater noise of whale-watching boats and potential effects on killer whales (*Orcinus orca*), based on an acoustic impact model." Marine Mammal Science 18 (Apr 2002): 394-418.
- Garcia, J.F., LT, USN. "Assessing the Performance of Omni-Directional Receivers for Passive Acoustic Detection of Vocalizing Odontocetes: Initial Analysis." Naval Postgraduate School, 2002.
- Hager, Carl Allen. "Modeling the Performance of the Pt Sur Hydrophone Array in Localizing Blue Whales." Naval Postgraduate School Master's Thesis, 1997.
- Medwin, H., and C.S. Clay. Fundamentals of Acoustical Oceanography. New York: Academic Press, 1998.
- Miller, C.W. and A. Kumar, "San Clemente Island undersea range acoustic experiment, July 2002," Naval Postgraduate School Technical Report, 2003.
- Ocean Noise and Marine Mammals. Committee on Potential Impacts of Ambient Noise in the Ocean on Marine Mammals, National Research Council. Washington, D.C.: The National Academies Press, 2003.
- Orr, Robert T. Marine Mammals of California. Los Angeles, CA: University of California Press, 1972.
- Purvis, P.E. and G.E. Pilleri. Echolocation in Whales and Dolphins. New York, NY: Academic Press Inc, 1983.
- Rago, Tarry. OC3260/OC4270 CTD and salts environmental analysis, July 2002. [<http://www.oc4270/Ju;y02/spray.nps.navy.mil>]. Feb 2003

Richardson, W. John, Charles R. Greene, Jr., Charles I. Malme, and Denis H. Thomson. Marine Mammals and Noise. San Diego, CA: Academic Press, 1995.

Tolstoy, Alexandra. Matched Field Processing for Underwater Acoustics. River Edge, NJ: World Scientific Publishing Co. Pte. Ltd., 1993.

Urick, R.J. Principles of Underwater Sound. New York: McGraw-Hill Book Company: New York, 1983.

Wenz, G.M. "Acoustic Ambient Noise in the Ocean: Spectra and Sources." Journal of the Acoustical Society of America 34 (1962) 1936-1954.

INITIAL DISTRIBUTION LIST

1. Defense Technical Information Center
Ft. Belvoir, VA
2. Dudley Knox Library
Naval Postgraduate School
Monterey, CA
3. Dr. Ching-Sang Chiu
Department of Oceanography
Naval Postgraduate School
Monterey, CA
4. Dr. Curtis A. Collins
Department of Oceanography
Naval Postgraduate School
Monterey, CA
5. Dr. Frank V. Stone
CNO (N45)
Arlington, VA
6. Prof. John Hildebrand
Scripps Institute of Oceanography
University of California, San Diego
La Jolla, CA
7. Mr. Chris Miller
Department of Oceanography
Naval Postgraduate School
Monterey, CA
8. Mr. Anu Kumar
Geo-Marine Incorporated
Newport News, VA